

Waterborne Latex with Renewable Oil Sources

Sara Filipa Leal Pinto

Final Dissertation submitted to

Escola Superior de Tecnologia e Gestão

Instituto Politécnico de Bragança

for obtain the master's degree in

Chemical Engineering

December 2014

Waterborne Latex with Renewable Oil Sources

Sara Filipa Leal Pinto

Final Dissertation submitted to

Escola Superior de Tecnologia e Gestão

Instituto Politécnico de Bragança

for obtain the master's degree in

Chemical Engineering

Oriented by:

Professor Rolando Carlos Pereira Simões Dias
Professor María J. Barandiaran

December 2014

The experimental part of this work was held in Institute of Polymer Materials (POLYMAT) part of The University of Basque Country in San Sebastián, Spain.

Dedicated to my parents, for all the love, dedication and strength they gave me through all my life.

Acknowledgements

I would like to express my sincere gratitude to Dr. Rolando Dias, for your friendship and knowledge, and for the opportunity to integrate me in the POLYMAT group.

I would like to express my gratitude to my supervisor Dr. María Barandiaran, for giving me the opportunity of doing this work in her research group. Without her support it would have been impossible to carry out this project.

Special thanks to Ana Fernandes, Jessica Desport and Mónica Moreno, for their help, guidance, patience and knowledge until the end of my training in San Sebastian. Thank you for everything.

I would like to thank all my colleagues in POLYMAT for their availability, scientific knowledge and friendship.

To my big friends Joana Lima, Catarina Gomes and Eliana Órfão a very special thanks for the amazing friendship during this 6 years. Thank you for the support, for the patience and for the friendship. Thank you for everything.

To all of my professors in Instituto Politécnico de Bragança, and Institute of Polymer Materials (POLYMAT) in San Sebastian, thank you for your support and motivation.

Aos meus pais e irmãos devo uma enorme gratidão pela compreensão, incentivo, preocupação, força e coragem e pelo que me puderam sempre proporcionar mesmo estando longe.

Abstract

The synthesis of polymers from renewable resource monomers is receiving an increasing attention, due to the high price and future depletion of fossil fuels, together with the concerns regarding environmental sustainability. Among the existing renewable raw materials, vegetable oils appear as one of the most interesting alternatives for the chemical and polymer industry.

Sunflower is grown in large extent in the Mediterranean basin, being Spain and Portugal ones of the major producing countries. Therefore, this vegetable oil can be considered as a promising candidate as a biobased starting material.

Besides, any progress towards sustainability achieved by the use of renewable feedstocks will be greatly improved by the use of a solvent-free environmentally friendly technology, such as emulsion polymerization.

Thus, the aim of this project is to synthesize waterborne polymers based on sunflower oil and probe their potential as binders for the coating industry. Sunflower oil is a triglyceride, which main components are oleic acid (C18, one unsaturation, 25% aprox) and linoleic (C18, two non-conjugated unsaturations, 65 % aprox). Those double bonds are not reactive enough for effective free radical polymerization, so the incorporation of polymerizable moiety, such as acrylic or vinyl groups, must be achieved.

In the first part of this project the synthesis of the sunflower oil macromonomer (SFOM) was studied. Stable latexes with considerable solids content were synthesized and miniemulsion polymerization was the technique used for the synthesis of the latex. The resulting polymer latex was analyzed in terms of conversion, particle size and microstructural properties. Furthermore the mechanical properties of the dried films were presented.

Keywords: Sunflower oil, fatty acids, miniemulsion polymerization

Resumo

A síntese de polímeros a partir de monómeros de recursos renováveis está a receber uma atenção crescente, devido ao elevado preço e futuro decréscimo dos combustíveis fósseis, juntamente com as preocupações em relação à sustentabilidade ambiental. Entre as matérias-primas renováveis existentes, os óleos vegetais, aparecem como uma das alternativas mais interessantes para a indústria química e de polímeros.

O girassol cresce em grande escala na bacia do Mediterrâneo, sendo Espanha e Portugal dois dos principais países produtores. Portanto, este óleo vegetal pode ser considerado como um candidato promissor como um material de partida de base biológica.

Além disso, qualquer avanço no sentido da sustentabilidade alcançada através da utilização de matérias-primas renováveis será grandemente melhorado pela utilização de uma tecnologia ambientalmente amigável, isento de solventes, tal como a polimerização em emulsão.

Assim, o objetivo deste projeto é a síntese de polímeros à base de óleo de girassol e investigar o seu potencial como agentes de ligação para a indústria de revestimentos. O óleo de girassol é um triglicerídeo, cujos componentes principais são o ácido oleico (C18, uma insaturação, aproximadamente 25%) e ácido linoleico (C18, duas insaturações não conjugadas, 65% aproximadamente). Estas duplas ligações não são suficientemente reativas para uma eficaz polimerização por radicais livres, assim a incorporação de uma mistura mais polimerizável, tal como grupos acrílicos ou vinílicos deve ser alcançada.

Na primeira parte deste projeto foi estudada a síntese do macromonómero de óleo de girassol (SFOM). Emulsões estáveis com um conteúdo de sólidos considerável foram sintetizadas e a polimerização em miniemulsão foi a técnica utilizada para a síntese do látex. O látex resultante foi analisado em termos de conversão, tamanho de partícula e propriedades microestruturais. Para além disso, as propriedades mecânicas dos filmes secos foram apresentadas.

Palavras-chave: Óleo de girassol, ácidos gordos, polimerização em miniemulsão.

Contents

Chapter 1	7
1.1. Introduction	7
1.2. Objectives	8
1.3. Dissertation structure	9
Chapter 2	10
Bibliographic revision	10
2.1. Monomers from renewable resources	10
2.2. Vegetable oils	11
2.3. Fatty Acids	13
2.4. Emulsion and miniemulsion polymerization	15
2.4.1 Emulsion polymerization	15
2.4.2 Miniemulsion Polymerization	16
Chapter 3	20
3.1. Experimental procedure for the synthesis of SFOM	20
• Monomer Characterization	22
3.2. Results and discussion	24
Chapter 4	28
4.1. Experimental procedure for Miniemulsion Polymerization	28
4.1.1. Miniemulsification	28
4.1.2. Miniemulsion Polymerization	29
4.1.3. Characterization	30
4.2. Results and discussion	32
4.2.1 Miniemulsification	32
4.2.2 Miniemulsion Polymerization	35
• Reproducibility of the reactions	39
• Gel content and Tg	41
4.3. Mechanical properties	42
Chapter 5	48
Conclusions	48
Future work	48
Bibliographic References	50

Index of Figures

Figure 1 - Raw materials precursors of renewable resource monomers and polymers. ^[11]	11
Figure 2 - Triglyceride structure of the vegetable oils (R1, R2, R3 represent fatty acid chains). ^[3]	11
Figure 3 - Different functionalities sites of a triglyceride molecule. ^[17]	13
Figure 4 - Representative scheme of emulsion polymerization.	16
Figure 5 - Sonication Process. ^[8]	17
Figure 6 - Homogenization valve of a Manton-Gaulin homogenizer.	18
Figure 7 – Miniemulsion polymerization process.....	19
Figure 8 - First Step of the synthesis of SFOM. MA added to the SFO.	20
Figure 9 - Second step of the synthesis to obtain the sunflower oil monomer.....	21
Figure 10 - Sunflower oil monomer final structure when MA react in both active sites of the triglyceride.	22
Figure 11 - ¹ H-NMR spectra corresponding to SFO.....	23
Figure 12 - ¹ H-NMR spectra of the step one of the synthesis A. Maleic anhydride was added to the SFO. 1) 0 hours; 2) 24 hours.	24
Figure 13 - Evolution of SFO functionalization with MA by 1H-NMR for the three synthesis. 25	
Figure 14 - ¹ H-NMR spectra of the final monomer (ASFOM).	26
Figure 15 - ¹ H-NMR structures for three final monomers. 1) Synthesis A; 2) Synthesis B; 3) Synthesis C.....	27
Figure 16 - Scheme for miniemulsion preparation method.....	29
Figure 17 - Scheme of soxhlet extraction method for gel content.	31

Figure 18 - Effect of the high pressure homogenization in the droplet size distribution of the miniemulsion for the synthesis A, B and C, respectively.	33
Figure 19 - Miniemulsion of CSFOM4 after sonication and homogenization, respectively.	33
Figure 20 - Effect of the high pressure homogenization in the droplet size distribution of the miniemulsion for the synthesis B and C, respectively.	34
Figure 21 - Effect of the high pressure homogenization in the droplet size distribution of the miniemulsion for the homopolymerization.	35
Figure 22 - Coagulum in the reactor and in the agitator (PCSFOM4).	36
Figure 23 - Evolution of the conversion and the particle size for the polymers PASFOM1 and PBSFOM2 respectively.....	36
Figure 24 - Evolution of the conversion and the particle size for the polymers PCSFOM4.....	36
Figure 25 - 1H-NMR spectra's of PBSFOM4 polymerization at different reaction times. 1) 0 minutes; 2) 120 minutes; 3) 240 minutes.	37
Figure 26 - Evolution of the conversion and the particle size for the polymers PBSFOM3 (ratio 65:35) and PCSFOM5 (ratio 50:50), respectively.....	38
Figure 27 - Evolution of the conversion and the particle size for the homopolymer PCSFOM6.	38
Figure 28 - Final aspect of latexes.	39
Figure 29 - Reproducibility of PBSFOM2 (ratio 70:30), for the conversion and for the particle size, respectively.	39
Figure 30 - Reproducibility of PBSFOM2 (ratio 65:35), for the conversion and for the particle size, respectively.	40
Figure 31 - Reproducibility of PBSFOM4, for the conversion and for the particle size, respectively.	41
Figure 32 - Primary auto-oxidation reaction mechanism.	43
Figure 33 - Secondary auto-oxidation reaction mechanism.	43

Figure 34 - Pictures of the films corresponding to the synthesis A, B and C, respectively.	44
Figure 35 - Pictures of the films corresponding to the synthesis B and C, respectively.	45
Figure 36 – Picture of the homopolymer PCSFOM6.....	45

Index of tables

Table 1 - Properties and fatty acid compositions of the most common vegetable oils. ^[3]	12
Table 2 - Most common fatty acids present in vegetable oils. ^[12]	14
Table 3 - Formulations employed in the synthesis of the SFOM.....	22
Table 4 - Synthesis performed and corresponding ratios of SFO and MA.	24
Table 5 - Unreacted double bonds for the final monomers.	25
Table 6 - General miniemulsion formulation.	28
Table 7 - Droplet size after the homogenization devices (Ratio SFOM:BA 70:30)	33
Table 8 - Different ratios of SFO: BA and droplet size after the homogenization devices.	34
Table 9 - Summary of the final results obtained for the miniemulsions formulations employed.	35
Table 10 – Final droplet size and conversion for the PBSFOM2.....	40
Table 11 - Final droplet size and conversion for the PBSFOM3.	40
Table 12 - Final droplet size and conversion for the PCSFOM4.	41
Table 13 - Gel content for the latexes studied.	42
Table 14 - Mechanical properties for all the latexes.	46

Nomenclature

AsA – Ascorbic acid

BA – Butyl acrylate

BTC – Benzene tricarboxylic acid

CDCl₃ – Deuterated chloroform

CMC – critical micelle concentration

DABCO – 1,4 – diazobicyclo [2.2.2] octane

dd – Droplet size

DMF - Dimethylformamide

DSC - Differential Scanning Calorimetry

dp – Particule size

D₂O – Deuterated water

IV – Iodine Value

M_w – Weight-average molecular weight

NaHCO₃ – Sodium Bicarbonate

N₂ – Nitrogen

ppm - Parts per million

¹H-NMR - Proton Nuclear Magnetic Resonance Spectroscopy

SC – Solid contents

TBHP – Tert-butyl hydroperoxide

T_g – Glass transition temperature (°C)

THF – Tetrahydrofurane

VOMM – Vegetable oils macromonomers

wbm% - Percentage based on monomer weight

wt% – Total weight percentage

[X_{SFOM}] – Fractional conversion of the sunflower oil monomer

[SFOM] – Concentration of the sunflower oil monomer

2-HEA – 2-hydroxyethyl acrylate

Chapter 1

1.1. Introduction

The synthesis of polymers from renewable resource monomers, such as oils and fats of vegetable and animal origin^[1], is receiving an increasing attention, due to the high price and future depletion of fossil fuels, together with the concerns regarding environmental sustainability.^[2] These materials make up the greatest proportion of current consumption of renewable raw materials in chemical industry, since they offer to chemistry a large number of possibilities for applications which can be rarely met by petrochemistry.^[1]

Recently, a variety of vegetable oil-based polymers have been prepared by free radical, cationic, olefin metathesis and condensation polymerization. The polymers obtained display a wide range of thermo physical and mechanical properties from soft and flexible rubbers to hard and rigid plastics, which show promise as alternatives to petroleum-based plastics.^[3] The replacement of petroleum-based raw materials by renewable resources constitutes a major contemporary challenge in terms of both economic and environmental aspects. This is why the natural vegetable oils are the most important class of renewable sources.

Larock and coworkers^[4] investigated polymeric systems based on vegetable oils such as soybean and tung oil that have been developed using a variety of polymerization techniques, including free radical, cationic, olefin metathesis and condensation polymerization, showing that some of these polymers present good properties compared to conventional petroleum-based polymers, and may serve as replacements for them.^[3] Because of the wide variety of possibilities for chemical transformations, universal availability and low price, oils and fats of vegetable and animal origin are preferred by the chemical industry as an alternative to fossil fuels.

Polymers from vegetable oils can generally be prepared by three strategies: (i) the direct polymerization through the double bonds or other reactive functional groups present in the fatty acid chain, (ii) the chemical modification of the double bonds to introduce easily polymerizable functional groups, and (iii) the chemical transformation of vegetable oils

to produce platform chemicals that can be utilized to prepare monomers for polymer synthesis.^[5]

Several authors are trying to modify these materials in order to synthesize several different monomers for use in structural applications. *Khot et al*^[6] study several pathways to synthesize monomers from triglycerides (in this case, soybean oil).

During the last decade, a variety of vegetable oil-based polymeric systems have been developed. Unmodified vegetable oils have been used to prepare biorenewable polymers^[3] by different polymerization methods, taking advantage of the carbon-carbon double bonds in the fatty acid chains.

Linseed, sunflower, castor, soybean, oiticica, palm and rapeseed oils are among the most used vegetable oils for the preparation of oil-modified polymers.^[7]

In this work, the chemical functionalization of the sunflower oil (SFO) through the double bonds (introducing polymerizable groups) were accomplished.

To carry out the free radical emulsion polymerization of the vegetable oil macromonomer is required a minimum water solubility to transport the monomer through the water phase from the monomer droplets to the polymer particles where the polymerization takes place. This represents a limitation in the case of vegetal oil macromonomer, such as sunflower oil macromonomer, because it possesses extremely low water solubility. The solution to this problem was to carry out a miniemulsion polymerization, mainly because diffusion limitations are avoided by polymerizing inside monomer droplets. To ensure droplet nucleation, small monomer droplets (50–500 nm) are formed and protected from diffusional degradation and droplet coagulation by using an efficient cosurfactant.^[8,9]

1.2. Objectives

In this work, the functionalization of sunflower oil (SFO) will be performed. After the functionalization, a mixture of SFOM and butyl acrylate will be copolymerized by miniemulsion.

The importance of keeping the unsaturation of the oleic acid during the synthesis, as well as the addition of drier (2 wbm %), on the improvement of the film properties will be analyzed.

1.3. Dissertation structure

The first chapter of this work aims to provide a perspective of the importance of vegetable oils in chemical and polymer industry due to the depletion of fossil fuels. The concerns regarding environmental sustainability will be referred as well.

Some bibliographical references on vegetable oils and fatty acids are discussed in chapter 2. Theoretical concepts associated to emulsion and miniemulsion polymerization will also be described.

In the third chapter, is presented the experimental procedure for the monomer synthesis as well as the results obtained and their discussion.

The chapter 4, besides the experimental procedure for all the miniemulsion polymerization process, it is also presented the main results and discussion. The mechanical properties of the films will be presented and discussed as well.

In chapter 5 the main conclusions of the work are presented and finally, the bibliographic references are presented.

Chapter 2

Bibliographic revision

In this chapter is presented a brief revision about vegetable oils and their structure, the fatty acids. Their reactive functionalities will be also mentioned. Some brief aspects about emulsion and miniemulsion polymerization will be referred as well.

2.1. Monomers from renewable resources

The use of renewable raw materials can significantly contribute to a sustainable development, usually interpreted as “acting responsibly to meet the needs of the present without compromising the ability of future generations to meet their own needs”.^[10] In ages of depleting fossil oil reserves and an increasing emission of greenhouse gases it is obvious that the utilization of renewable raw materials wherever and whenever possible is one necessary step towards a sustainable development. In particular, this can perennially provide a raw material basis for daily life products and avoid further contribution to greenhouse effects due to CO₂ emission minimization.^[2]

A renewable resource is defined, in this context, as any animal or vegetable species which is exploited without endangering its survival and which is renewed by biological (short term) instead of geochemical (very long term) activities.^[11] For example, plant oils offer many advantages apart from their renewability. Their world-wide availability and relatively low prices make them industrially attractive and feasible, as daily demonstrated with industrial oil chemistry^[12] as well polysaccharides (mainly cellulose and starch), sugars, wood and others. Pharmaceuticals, coatings, packaging materials or fine chemicals are some of the possible applications of these products.^[2]

Figure 1 summarizes the main existing renewable raw materials as precursors of monomers and polymers. They can be divided in three principal categories according to their origin: vegetal, animal or produced by bacteria.^[11]

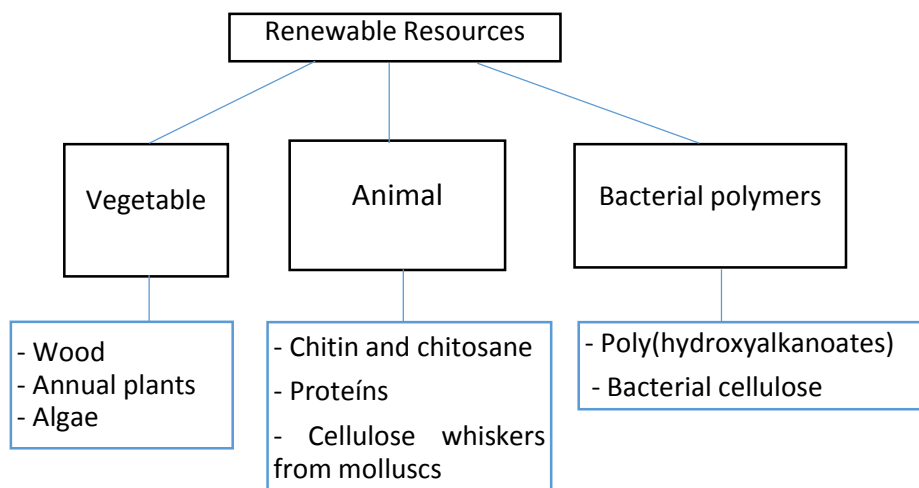


Figure 1 - Raw materials precursors of renewable resource monomers and polymers.^[11]

Although there are a broad range of natural resources in nature, vegetable oils are one of the features that are revolutionizing the chemical and polymer industry, due to their biodegradability, low toxicity, easy availability, relatively low price and shortage of organic chemicals emissions.^[13]

2.2. Vegetable oils

Chemically, vegetable oils consists of mainly triglycerides formed between glycerol and various fatty acids, as shown in Figure 2.^[3]

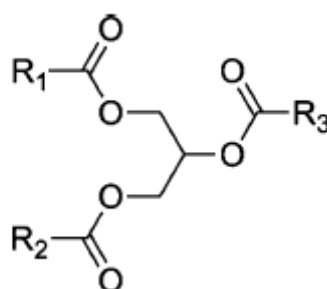


Figure 2 - Triglyceride structure of the vegetable oils (R1, R2, R3 represent fatty acid chains).^[3]

Different vegetable oils contain different composition of fatty acids depending on the plant and the growing conditions. The fatty acid compositions of the most common

vegetable oils are summarized in Table 1.^[3] The chain length of the fatty acid and the number and position of the unsaturation determines the physical and chemical properties of the oil.^[11], which can be determined by measuring the iodine value (IV). This value represents the amount of iodine (mg) that reacts with the carbon–carbon double bonds in 100 g of vegetable oil; the larger IV value indicates more carbon–carbon double bonds per vegetable oil triglyceride.^[3] Thus, vegetable oils are divided into three groups depending on their iodine values. They are classified as ‘drying’, if their iodine value is higher than 130, ‘semidrying’ if this parameter is comprised between 90 and 130 and ‘non-drying’ when it drops below 90.^[11]

Hence, the presence of unsaturated acids in vegetable oils provides them with the important commercial property of “drying”,^[14] i.e. the double bonds of the unsaturated acids react with atmospheric oxygen and then with one another to form a three-dimensional polymeric network.^[15]

Table 1 - Properties and fatty acid compositions of the most common vegetable oils.^[3]

Vegetable oil	Double bonds ^a	Iodine value ^b /mg per 100 g	Fatty acids (%)				
			Palmitic	Stearic	Oleic	Linoleic	Linolenic
Palm	1.7	44–58	42.8	4.2	40.5	10.1	—
Olive	2.8	75–94	13.7	2.5	71.1	10.0	0.6
Groundnut	3.4	80–106	11.4	2.4	48.3	31.9	—
Rapeseed	3.8	94–120	4.0	2.0	56.0	26.0	10.0
Sesame	3.9	103–116	9.0	6.0	41.0	43.0	1.0
Cottonseed	3.9	90–119	21.6	2.6	18.6	54.4	0.7
Corn	4.5	102–130	10.9	2.0	25.4	59.6	1.2
Soybean	4.6	117–143	11.0	4.0	23.4	53.3	7.8
Sunflower	4.7	110–143	5.2	2.7	37.2	53.8	1.0
Linseed	6.6	168–204	5.5	3.5	19.1	15.3	56.6

^a Average number of double bonds per triglyceride. ^b The amount of iodine (mg) that reacts with the double bonds in 100 g of vegetable oil.

The natural abundance and reactive functionalities of vegetable oils make them useful oil chemicals for polymer chemistry. The triglyceride molecules have several active sites such as the double bonds (1), the allylic carbons (2), the ester groups (3) and the alpha carbon (4), as showed in Figure 3.^[16] Typical modifying reactants include maleic acid, maleic anhydride, methacrylic acid, and acrylic acid.^[17]

The most widely used vegetable oils as macromonomers for the synthesis of polymeric materials are soybean oil, linseed oil, sunflower oil and tung oil.^[6, 4]

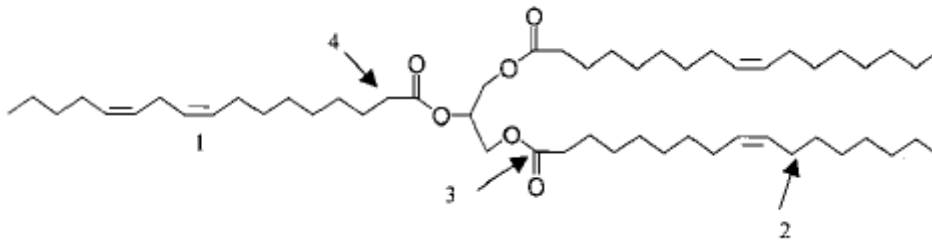


Figure 3 - Different functionalities sites of a triglyceride molecule.^[17]

Because of low reactivity of their unsaturated aliphatic chains makes them ineffective monomers when used as such. This drawback can be overcome by functionalizing them with polymerizable moieties, such as vinyl or acrylic groups^[16] in order to improve the polymerization process.

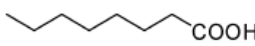
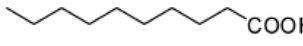
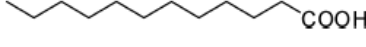

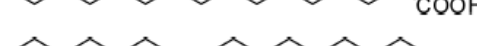
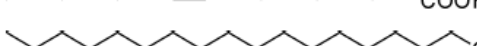
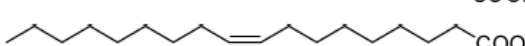
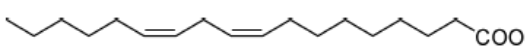
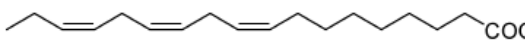
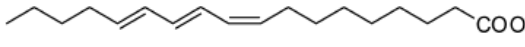
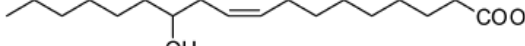
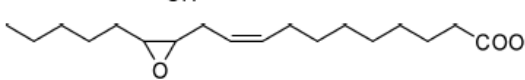
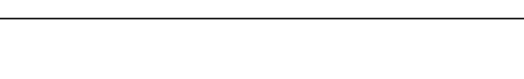
The chemical functionalization of vegetable oils have been studied, including acrylation, maleinization, epoxidation, hydroxymethylation, esterification and halogenation. This^[6,7] transformations (typical modifying reactants include maleic acid, maleic anhydride, methacrylic acid and acrylic acid) make triglyceride double bonds^[4] capable of reaction via ring opening^[6] and then react with a functional vinyl monomer to form the vegetable oil macromonomer.

2.3. Fatty Acids

Fatty acids account for 95% of the total weight of triglycerides and their content is characteristic for each plant oil. The formulas and structures of the most important fatty acids are represented in Table 2.

Among the several known fatty acids, oleic and linoleic acids can be considered as promising candidates to be used as bio-based starting materials. The reason behind this, is that they are the principal components of sunflower and olive oils, which are grown in large extent in the Mediterranean basin, being Spain one of the major producing countries.^[13]

Table 2 - Most common fatty acids present in vegetable oils.^[12]

Fatty Acid	Formula	Structure
Caprylic	$C_8H_{16}O_2$	
Capric	$C_{10}H_{20}O_2$	
Lauric	$C_{12}H_{24}O_2$	
Myristic	$C_{14}H_{28}O_2$	
Palmitic	$C_{16}H_{32}O_2$	
Palmitoleic	$C_{16}H_{30}O_2$	
Stearic	$C_{18}H_{36}O_2$	
Oleic	$C_{18}H_{34}O_2$	
Linoleic	$C_{18}H_{32}O_2$	
Linolenic	$C_{18}H_{30}O_2$	
α -Eleostearic	$C_{18}H_{30}O_2$	
Ricinoleic	$C_{18}H_{34}O_3$	
Vernolic	$C_{18}H_{32}O_3$	

The chain length of these fatty acids can vary from 14 to 22 carbons and contain 0–5 double bonds situated at different positions along the chain and in conjugated or unconjugated sequences.^[11]

The unsaturation of the fatty acids has traditionally been used for oxidative curing reactions leading to “air drying” of some plant oils. This is the chemistry of the well-known alkyd resins used for paint and varnish binders.^[17]

As mentioned before, the triglyceride molecule has many reactive sites. Since the double bonds of the sunflower oil are not sufficiently reactive for effective free radical polymerization, a much more reactive polymerizable moiety (such as acrylic or vinyl groups) must be incorporated into the chain, and thus improve the polymerization.

The degree of crosslinking dictates the shear, or cohesive, strength of the polymer. Monomers derived from plant oils possess an inherent degree of unsaturation that varies from plant to plant. The variation of unsaturation among the various plant oils, and hence the fatty acids, can be used as an advantage. Depending on the property desired in the final product, various oils, or mixtures thereof, may be used in synthesizing the monomers. Functional groups that increase adhesive strength can also be placed onto unsaturation sites.^[17]

2.4. Emulsion and miniemulsion polymerization

Most of the research carried out around the polymerization of vegetable oils and fatty acids is focused on solution polymerization.^[13] However, in emulsion and miniemulsion the polymerization process takes place in individual particles and the production of high molecular weight polymers at considerably higher polymerization rates is possible. This combination is not achieved in bulk and solution polymerization. Also emulsion and miniemulsion polymerization allows making products with special properties that other types of polymerization process such as bulk or solution are not able to produce.^[18]

2.4.1 Emulsion polymerization

Any progress towards sustainability achieved by the use of renewable feedstocks will be greatly improved by the use of a solvent-free environmentally friendly technology, such as emulsion polymerization. However, the hydrophobic nature of monomers coming from vegetable oils represents a challenge for their incorporation into emulsion polymerization.^[13] In this process the monomer is dispersed in an aqueous solution of surfactant whose concentration usually exceeds the critical micelle concentration (CMC).^[8] This will stabilize the monomer droplets, but due to the excess of the surfactant the rest is in the aqueous phase and it will form aggregates, known as micelles, as can be seen in Figure 4.^[18] After adding the initiator, the particles will start generating. In principle, polymer particles could be formed by entry of radicals into the micelles (heterogeneous nucleation), by radical entry into the monomer droplets, and by precipitation of growing oligomers in the aqueous phase (homogeneous nucleation). However, as the surface area of the micelles is relatively large compared to the monomer droplets, the probability of a radical enter into a monomer droplet is very low. This means that most of the particles are formed by either homogeneous or heterogeneous nucleation.^[8]

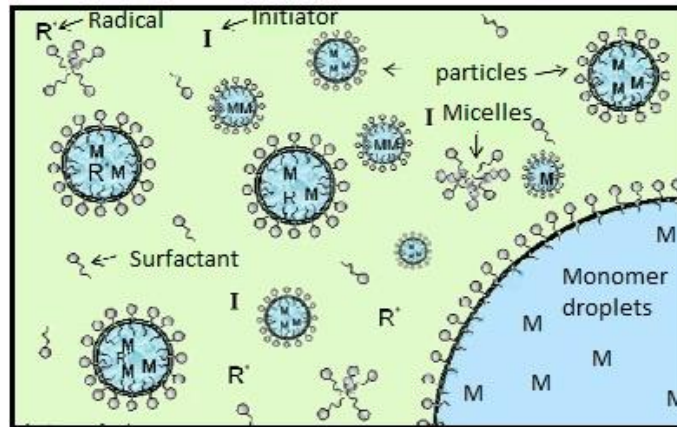


Figure 4 - Representative scheme of emulsion polymerization.

When particles are nucleated they grow by polymerization. The monomer required for polymerization must be transported from the monomer droplets to the polymer particles by diffusion through the aqueous phase. This represents a severe limitation in the case of hydrophobic monomers, as diffusion is precluded. The need of mass transport of monomer or other water insoluble compound through the aqueous phase would be greatly diminished if all, or at least a large fraction of the monomer droplets, were nucleated. Predominant droplet nucleation can only occur if the surface area of the monomer droplets is large compared to that of the micelles, and this requires submicron droplet sizes. To obtain submicron sizes, high energy homogenization should be applied and the droplets should be protected against coalescence and diffusional degradation by using a water insoluble compound such as hexadecane, and an efficient surfactant. These ideas are the basis of miniemulsion polymerization.^[13,8]

2.4.2 Miniemulsion Polymerization

There is a fundamental difference between traditional emulsion polymerization and a miniemulsion polymerization. Particle formation in the former is a mixture of micellar and homogenous nucleation; particles formed via miniemulsion however are mainly formed by droplet nucleation.^[8]

Miniemulsions are water-in-oil stable dispersions with a droplet size between 50-500 nm. These droplets must be protected against both diffusional degradation (Ostwald ripening) and droplet coagulation by using a water insoluble low molecular weight compound (costabilizer) and an efficient surfactant, respectively.

There are different methodologies to prepare the miniemulsions. Normally they are prepared in two steps. First, the monomer is dispersed in an aqueous solution of surfactant. At this time the droplets in the system have a relative stability (droplet size around 50 to 500 nm). Then, during the dispersion formation is necessary a high shear mechanism, in order to achieve a steady state between the rate of coalescing and breaking in the droplets (such as sonifiers and high pressure homogenizers). Finally the polymerization start by means of an initiator system (most often soluble in water), the droplets formed in the previous step are nucleated and polymerized without changing their characteristics.

- Homogenization Devices

A variety of equipment is commercially available for emulsification. The most important are rotor-stator systems, sonifiers and high-pressure homogenizers.

In this work the sonifier and the high-pressure homogenizer were used.

The sonifier produces ultrasonic waves that cause oscillation of the molecules about their main position as the waves propagate. The shock waves produce the total collapse of the bubbles causing the breakup of the surrounding monomer droplets. A problem associated with the sonifier is that only a small region of the fluid around the sonifier tip is directly affected by the ultrasound waves, as can be seen in Figure 5.

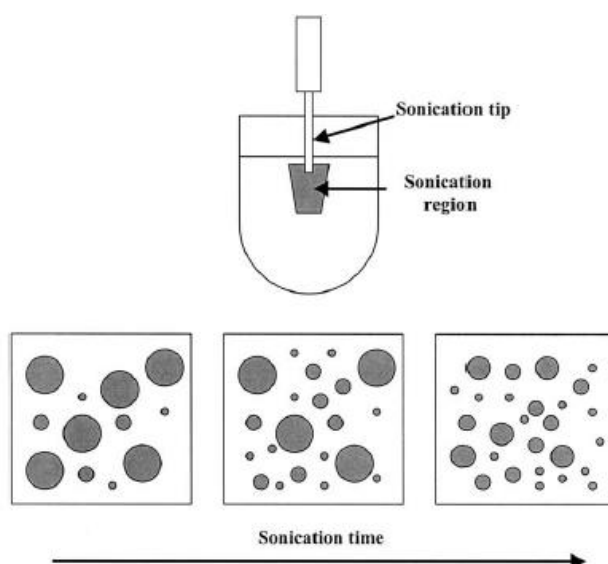


Figure 5 - Sonication Process.^[8]

In order to be broken up, the monomer droplets should pass through the sonication region. Therefore, when sonication is used to form the miniemulsion, additional stirring must be used to allow all the fluid to pass to the sonication region, allowing the mixture to reach a steady state. This process makes the miniemulsion characteristics dependent on the sonication time. Thus, there is evidence that droplet size decreases with time. The decrease is initially pronounced and later the droplet size evolves asymptotically towards a value that depends on both the formulation and the energy input.^[8]

The most commonly high pressure homogenizers used are the Microfluidizer and the Manton-Gaulin. Both of them have in common that coarse dispersions are pressurized using a positive displacement pump, and flow through a narrow gap at high velocity. A strong pressure drop also occurs.^[8]

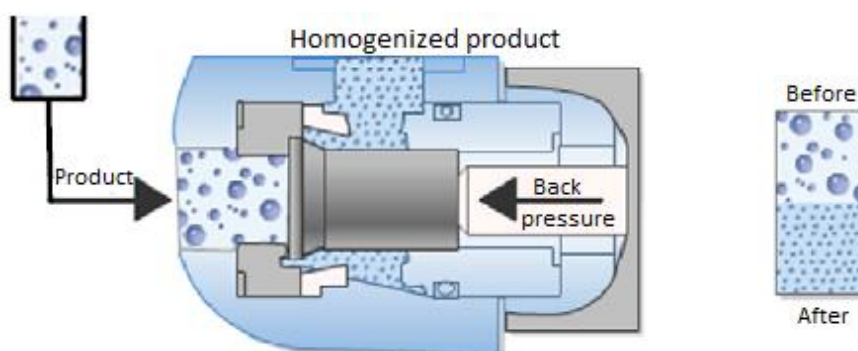


Figure 6 - Homogenization valve of a Manton-Gaulin homogenizer.

In high pressure homogenizers, the pre-emulsion is added in a feed recipient and pumped at low speed. As the valve is closed, the area where the fluid goes is reduced, increasing the system pressure. The fluid pass through a microchannel where the stream accelerate to approximately 300 m/s. Through the sudden pressure drop the big particles break in smaller particles. The uniformity and the diameter of the droplets can be adjusted through the pressure, number of cycles (liquid path by the bomb) and surfactant concentration.

Tacking to account that in an efficiently nucleated miniemulsion, the size of the final particles is close to the size of the initial droplets, miniemulsion polymerization allows a good control of the particle size and the particle size distribution, which is difficult to achieve emulsifying preformed polymers in water.

Figure 7 resume the different steps present in a miniemulsion polymerization process.

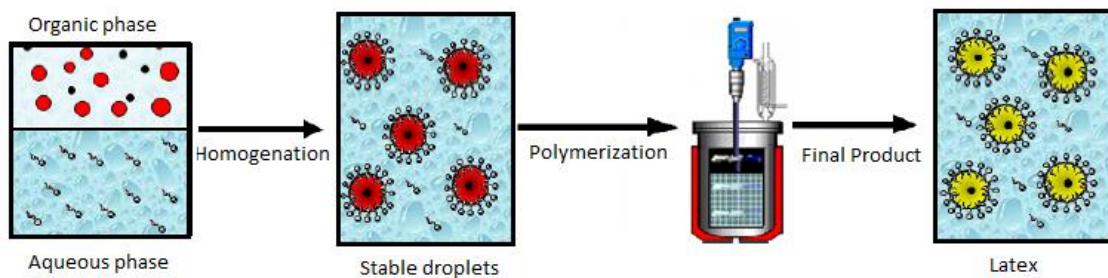


Figure 7 – Miniemulsion polymerization process.

Miniemulsion polymerization allows also the possibility to produce high solids content low viscosity latexes, important from an industrial, commercial and environmental point of view. The low viscosity of the latexes produced by miniemulsion comes from their polydispersity in the particle size distribution.^[19]

Chapter 3

In this chapter the experimental procedure for the synthesis of sunflower oil monomer (SFOM) will be presented. The results obtained and their brief discussion will be presented as well.

3.1. Experimental procedure for the synthesis of SFOM

Following the experimental procedure described by Black^[20], sunflower oil monomer synthesis was carried out in two steps. First, maleic anhydride (Fluka, purity $\geq 99.0\%$) reacted with the sunflower oil (Sigma Aldrich). Different synthesis were prepared varying the ratios of SFO/MA. The SFO was added into a 250 mL three necked round-bottom flask equipped with a nitrogen inlet, a condenser, and a thermocouple. The system was heated using a silicone bath until 165 °C. When the systems reached this temperature, MA was added and let it stirring for 24 hours (molar ratio used is based on the percentage of linoleic acid presented in SFO). The scheme of this step of the synthesis is shown in Figure 8.

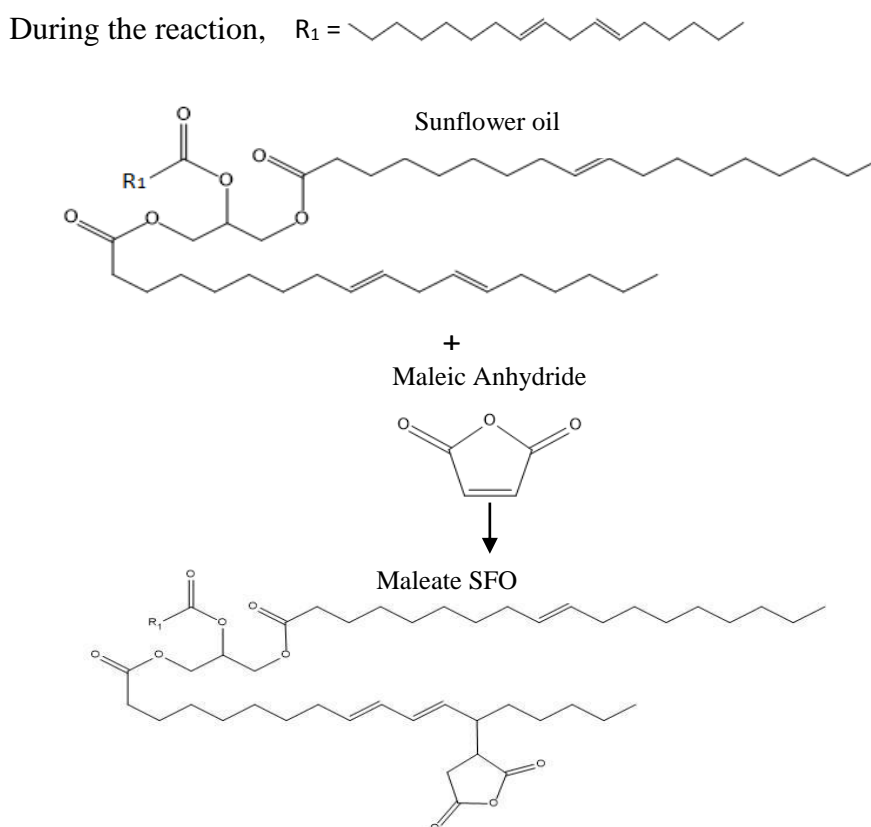


Figure 8 - First Step of the synthesis of SFOM. MA added to the SFO.

Then, the system was cooled to 60 °C and 2-hydroxyethyl acrylate (2-HEA), (Sigma Aldrich, purity 96%) and the catalyst 1,4-diazobicyclo [2.2.2]octane (DABCO) (Sigma Aldrich, purity 99%) were added to the previous mixture under continuous agitation during 4 hours. Figure 9 shows the second step of the monomer synthesis to obtain the sunflower oil monomer (SFOM).

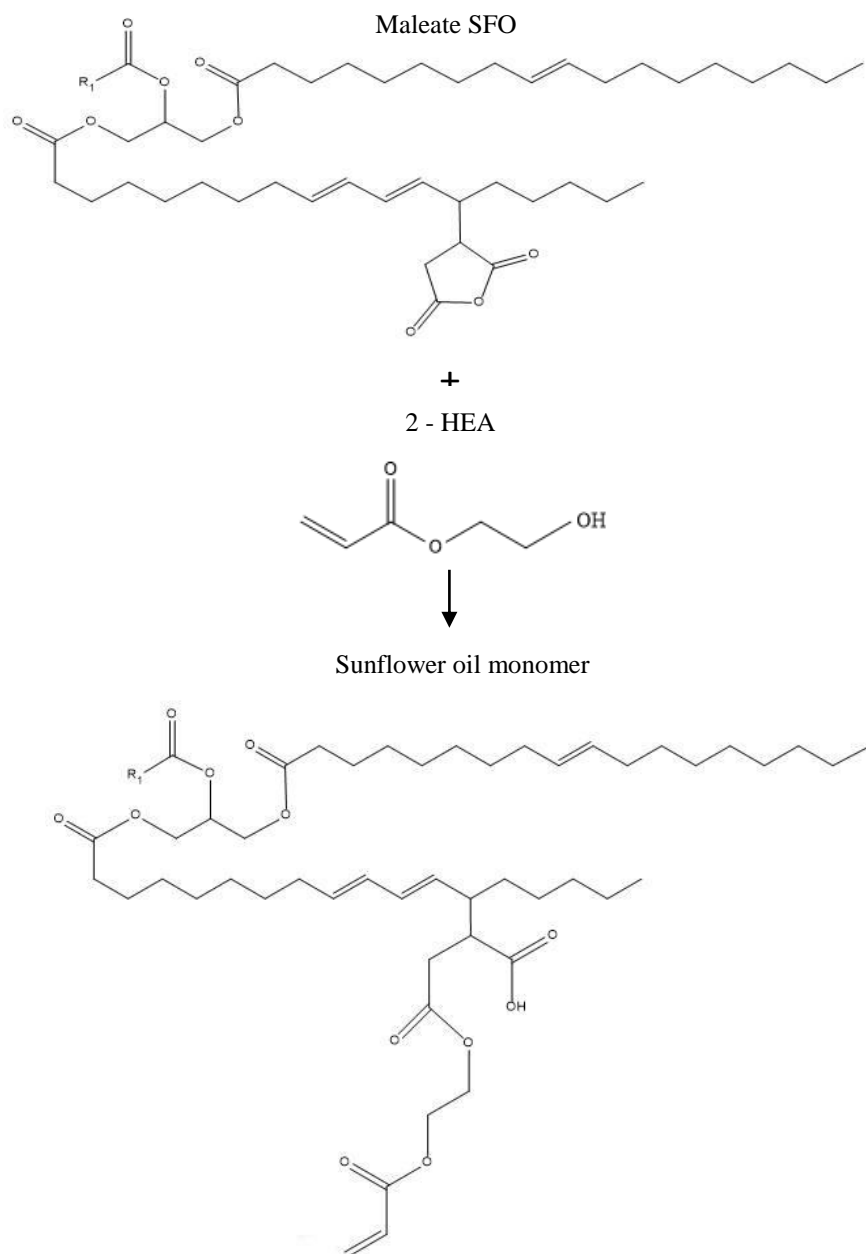


Figure 9 - Second step of the synthesis to obtain the sunflower oil monomer.

The triglyceride contains several active sites amenable to chemical modification, thus the maleic anhydride can also react in both active sites of the triglyceride. Figure 10 shows the other possible monomer structure.

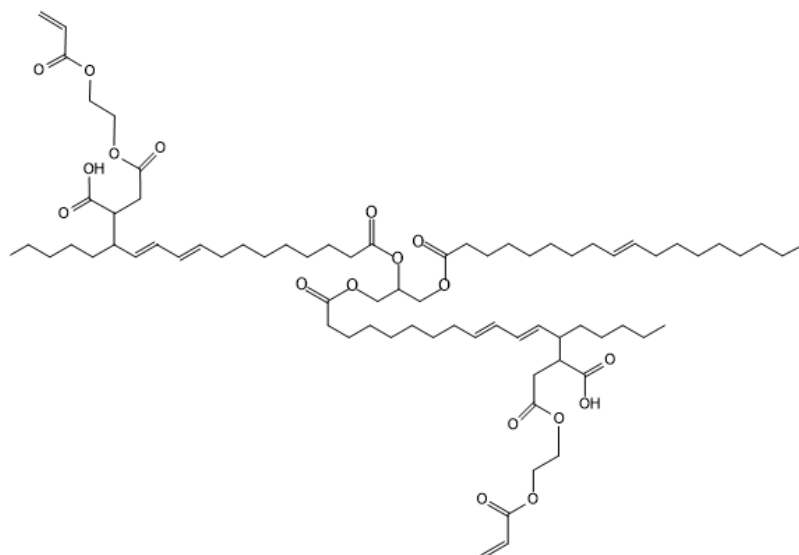


Figure 10 - Sunflower oil monomer final structure when MA react in both active sites of the triglyceride.

In Table 3 the formulation of all the synthesis performed is presented.

Table 3 - Formulations employed in the synthesis of the SFOM.

Compound	Synthesis A	Synthesis B	Synthesis C
	(1SFO:1MA)	(1SFO:1.5MA)	(1SFO:2MA)
	Amount (g)		
SFO	100,43	100,43	100,43
MA	11,18	16,81	22,34
2-HEA	13,24	19,87	26,48
DABCO (wt%) ¹	1,2484	1,3693	1,4925

¹ weight based on total weight.

- Monomer Characterization

To determine the functionalization degree of SFO and characterize the structure of the monomer, small amounts of reaction solution were extracted at different intervals of time and analyzed by ¹H-NMR spectroscopy. A Bruker DRX-500 spectrometer, 500 MHz was

used and the samples were dissolved in deuterated chloroform (CDCl₃). Figure 11 illustrates the ¹H-NMR spectra of SFO during the synthesis.

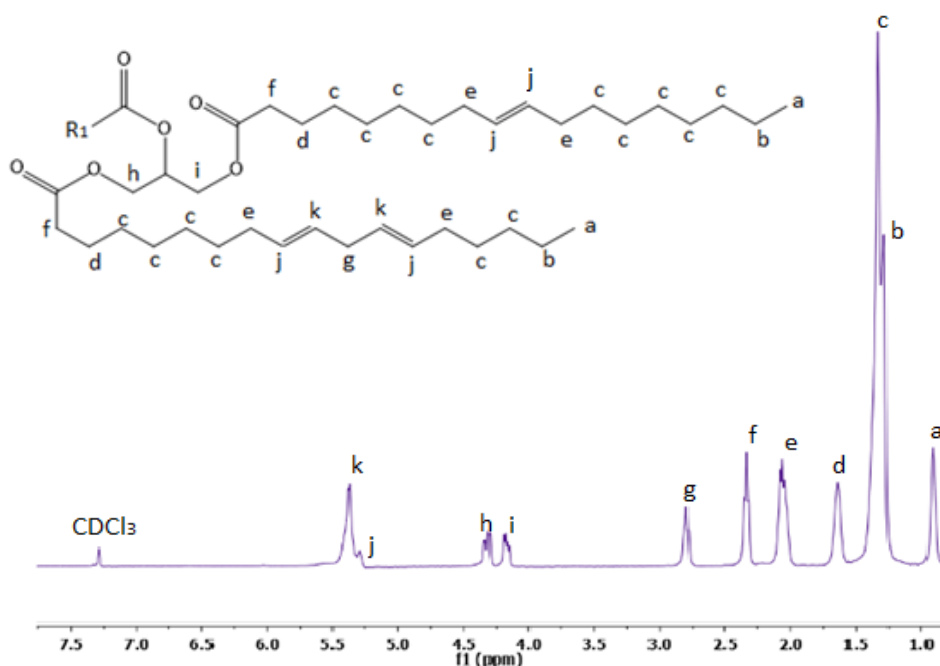


Figure 11 - ¹H-NMR spectra corresponding to SFO.

To determine the number of double bonds present in the SFOM structure before, during and after the functionalization with maleic anhydride, Iodide Value (IV) was calculated. To this end, samples were taken over time and analyzed by ¹H-NMR spectroscopy. Using the methods propose by Johnson and Schoolery^[21], IV parameter was calculated using the signal area of the olefinic (F) and total area hydrogen atoms (T) in the ¹H-NMR spectrum trough the following expression:

$$IV = \frac{12691F}{120.0 + 7.013T + 6.006F} \quad (1)$$

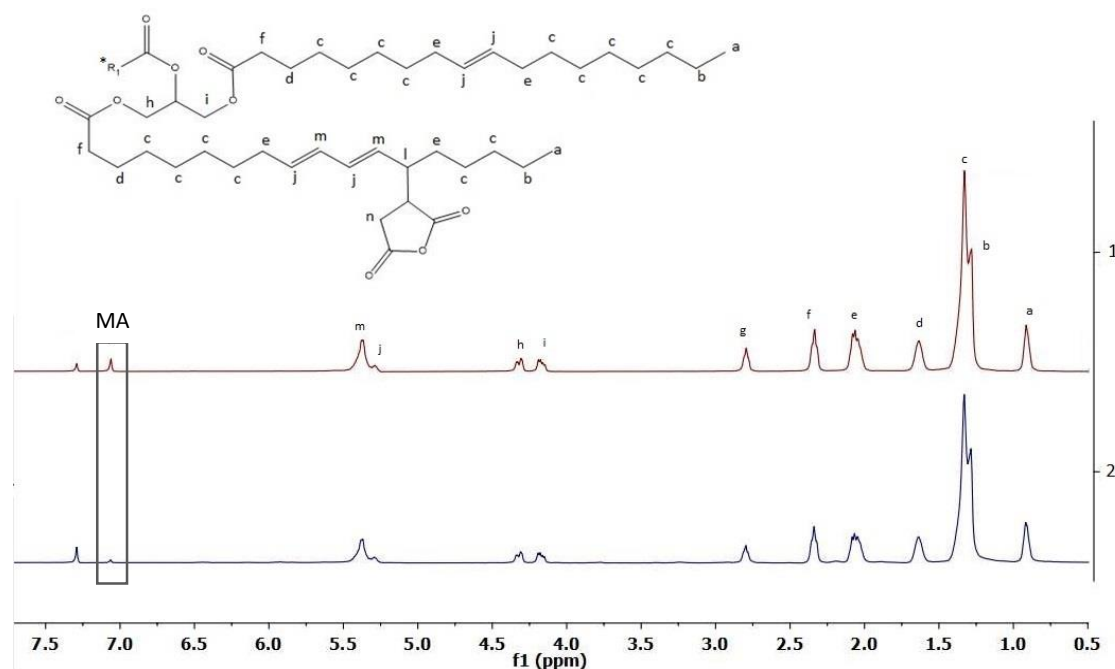
3.2. Results and discussion

Table 4 shows the different synthesis performed in this work.

Table 4 - Synthesis performed and corresponding ratios of SFO and MA.

Synthesis	Ratio (SFO:MA)
A	1:1
B	1:1.5
C	1:2

Figure 12 illustrates the $^1\text{H-NMR}$ spectra of the first step of the synthesis A, the addition of maleic anhydride to the sunflower oil, at the beginning and at the end of the reaction.



*R₁ represents the same chain where the maleic anhydride is reacting.

Figure 12 - $^1\text{H-NMR}$ spectra of the step one of the synthesis A. Maleic anhydride was added to the SFO. 1) 0 hours; 2) 24 hours.

In the spectrum, the main characteristic peaks are assigned. In the low field is the signal corresponding to the solvent (chloroform) (7.26 ppm) and the maleic anhydride (7.05 ppm), followed by the signals corresponding to the double bonds of the sunflower oil (5.21-5.54 ppm). Between 4.08 and 4.38 ppm were found the signals corresponding to the glyceryl protons group. The high field (0.77-2.77 ppm) is dominated by the alkyd chain protons of the oil.

During the 24 hours, samples were taken over time to observe the incorporation of the MA into the SFO chain.

It can be seen that the peak corresponding to the MA decrease with time, which shows that it is reacting and it is incorporated into the chain.

The same behavior was observed with the other synthesis.

In order to characterize the monomer and thus determine the double bonds present in the SFOM structure, IV (iodine value) was calculated. The Figure 13 shows the evolution of the IV over 24 hours of maleic anhydride's reaction for each synthesis. As can be seen, a decrease of the double bonds along the reaction was observed, indicating that the double bonds were reacting with the maleic anhydride.

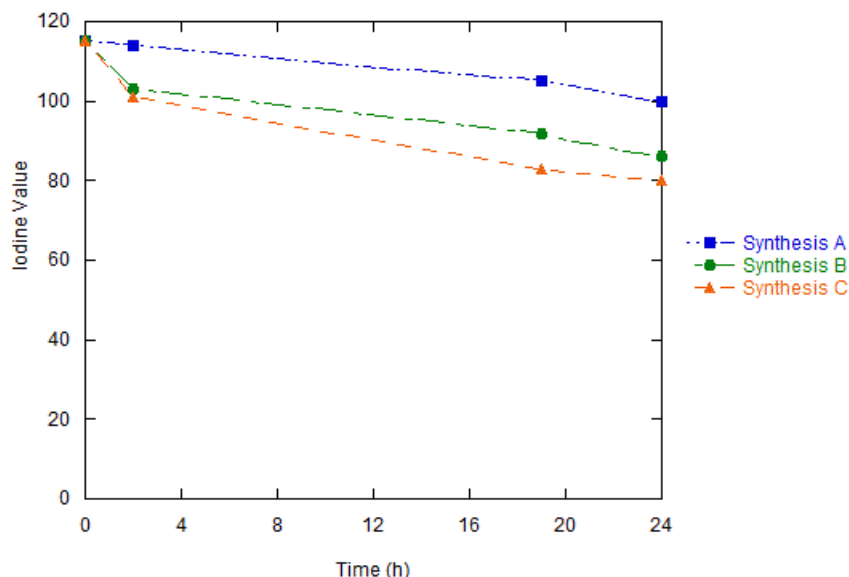


Figure 13 - Evolution of SFO functionalization with MA by 1H-NMR for the three synthesis.

In Table 5 is represented the final double bonds for each monomer, the unreacted double bonds.

Table 5 - Unreacted double bonds for the final monomers.

Synthesis	Ratio (SFO:MA)	Monomer	SFO (0h)	IV
A	1:1	ASFOM	115	100
B	1:1.5	BSFOM	115	86
C	1:2	CSFOM	115	80

As Table 5 shows, the higher the amount of MA added to SFO, more double bonds are going to react. Thus, in synthesis C, the amount of unreacted double bonds (IV) is lower than in the other synthesis.

The second step of the synthesis is the addition of 2-HEA and the catalyst to the previous solution for more 4 hours.

In Figure 14 is represented the $^1\text{H-NMR}$ spectra of the final monomer, sunflower oil monomer for the synthesis A. The main characteristic peaks are also assigned.

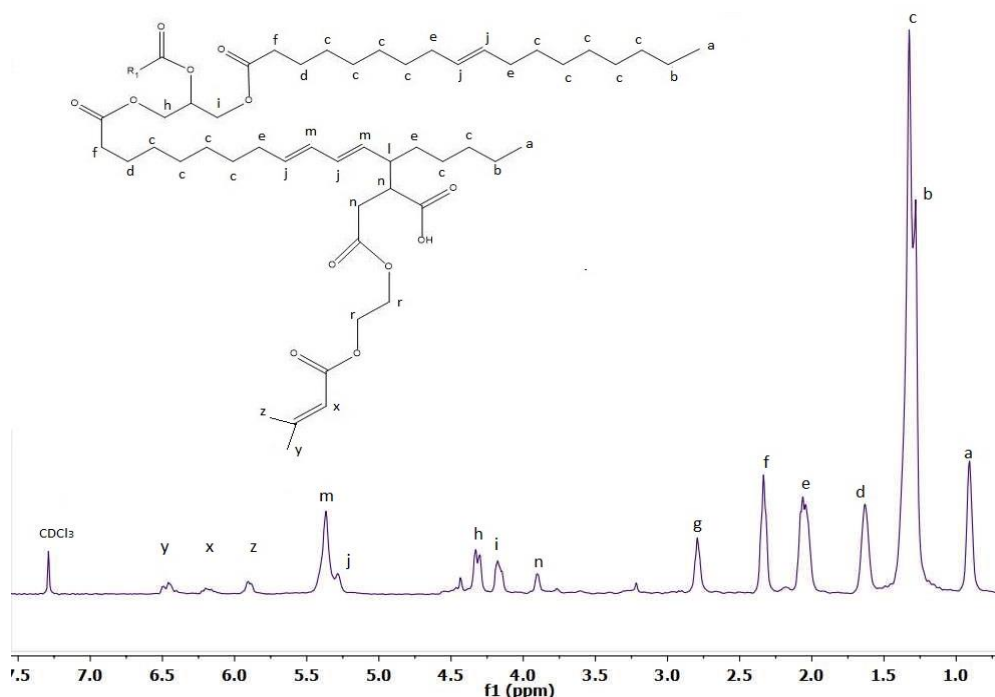


Figure 14 - $^1\text{H-NMR}$ spectra of the final monomer (ASFOM).

As can be seen through the Figure 14, new signals were detected, which can be shown by the letters z, x and y, corresponding to the vinyl protons of the 2-HEA (5.88, 6.15 and 6.45 ppm, respectively). These signals represent the three protons of the acrylate group on the monomer structure. Near to the glyceryl signals (h and i), appears a new multiplet (3.90 ppm), associated to the methylene protons between carbonyl groups (n).

The maleic anhydride signal disappears completely, which means that there is no evidence of unreacted maleic anhydride in the final monomer structure.

In the Figure 15 is represented by $^1\text{H-NMR}$ the final monomer structure of all the synthesis performed.

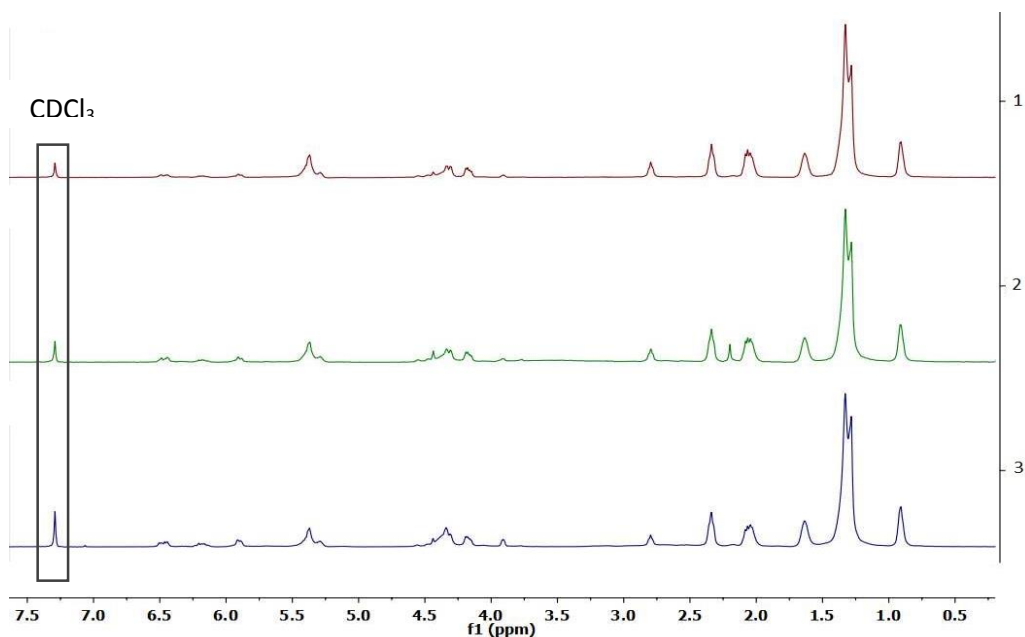


Figure 15 - $^1\text{H-NMR}$ structures for three final monomers. 1) Synthesis A; 2) Synthesis B; 3) Synthesis C.

Small differences between the final monomer structures can be observed. For instance, in Synthesis B, a small peak appears at 2.24 ppm, which doesn't happen in the other synthesis. This peak can be related to impurities present in the monomer process.

In synthesis C, a small peak next to the CDCl_3 which corresponds to the non-reacted maleic anhydride (7.06 ppm) is detected. This means that besides the monomer, there is also a small amount of unreacted MA in the system. Between the 3.75 to 4.5 ppm regions some irrelevant changes were observed, due to how the maleic anhydride reacts with the 2-HEA. In the acrylate region (5.86 to 6.56 ppm) it can be seen a slight intensity of the curves according to the amount of 2-HEA added.

After this step, all the 3 monomers are able to copolymerize via miniemulsion polymerization with butyl acrylate.

Chapter 4

This chapter will be related to all the experimental procedure for the miniemulsion polymerization process. The final latex properties will be presented, along with a brief discussion on the results obtained.

4.1. Experimental procedure for Miniemulsion Polymerization

4.1.1. Miniemulsification

All miniemulsions contained 30 wt% solids content, 4 wbm% (weight based on monomer weight) of nonionic surfactant (surfmer Reasop SR10, ADEKA), 1 wbm% of the redox pair tert butyl hydroperoxide (TBHP) (Sigma Aldrich, 70 wt% in H₂O)/ascorbic acid (AsA) (Fluka). NaHCO₃ (Sigma Aldrich, purity ≥99.7%) was added at a concentration of 0.039 M in the water phase to diminish electrostatic interactions between droplets.

The general formulation is shown in Table 6.

Table 6 - General miniemulsion formulation.

Ingredient	Amount (g)
SFOM	21
BA	9
Water	70
AsA ^a	0,3
TBHP ^a	0,3
NaHCO ₃ ^b	0,45
Surfmer ^c	1,2

^a1 wbm%, ^b 1,5 wbm%, ^c 4 wbm%

To produce the miniemulsions, the organic phase was added dropwise to the aqueous phase under continuous agitation. The resultant mixture were mixed by magnetic stirring during 30 minutes at 1600 rpm. After the agitation, the mixture was sonified in a Branson 450 equipment (15 min and 80 % duty cycle) under ice cooling and further treated with a high-pressure homogenizer (6 cycles) (Niro-Soavi, Panda 2K) using 60.0 MPa in the first valve and 6.0 MPa in the second stage valve.

In Figure 16 the scheme for the miniemulsion process is represented.

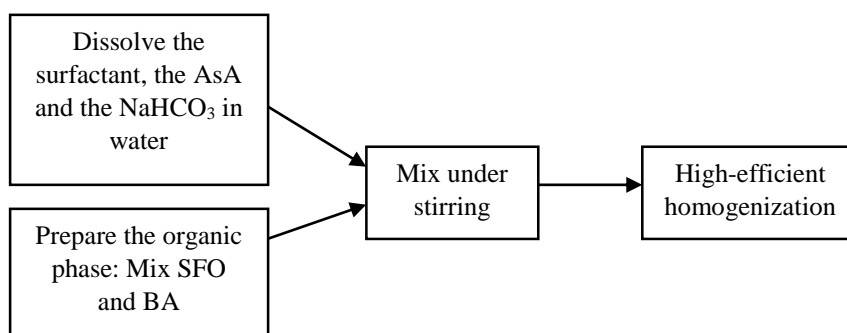


Figure 16 - Scheme for miniemulsion preparation method.

Miniemulsion polymerization usually requires the presence of a costabilizer to prevent monomer diffusion from smaller to larger droplets (Ostwald ripening)^[31,32], which in many cases are classified as volatile organic compounds.^[8] However, all the polymerizations reported in this work were performed in the absence of costabilizer, because, as it has been already reported^[9], the monomer itself, due to its low water solubility, was able to stabilize the miniemulsions.

The combination of sonication and high pressure homogenization has been proven to be very efficient to emulsify highly viscous and highly hydrophobic compounds. Furthermore, it has been demonstrated that the feeding of a non-phase separated preemulsion with small droplet size into the high pressure homogenizer allowed to obtain small droplets with quite narrow droplet size distribution at a smaller number of cycles.^[22, 28, 29, 30]

4.1.2. Miniemulsion Polymerization

The polymer latexes were synthesized by miniemulsion polymerization at 70 °C following the formulation showed on Table 6. The miniemulsions were carried out in the Miniplant M100 set-up in reactors of 100 mL equipped with a reflux condenser, sampling device, nitrogen inlet, a feed inlet tube and a stainless steel turbine-type stirrer rotating at 200 rpm.

The redox pair initiator was added in two stages. The reductant agent, ascorbic acid was added in the aqueous phase while the oxidant agent TBHP, was fed for 2 hours. After the feeding the system was allowed to react in batch for a further 2 hours. During all the reaction, samples were withdrawn over regular intervals to determine the monomer conversion. Hydroquinone was used to stop the reaction.

4.1.3. Characterization

The z-average diameters of miniemulsion droplets (dd) and latex particles (dp) were measured by dynamic light scattering (Zetasizer Nano ZS, Malvern Instruments). Samples were prepared by diluting a fraction of the miniemulsion or latex with deionized water.

To quantify the monomer concentration and therefore the monomer conversion during miniemulsion polymerization, ¹H-NMR spectroscopy (Bruker AVANCE spectrometer 500 MHz) was used. Benzenetricarboxylic acid (BTC) (Sigma-Aldrich) was used as internal standard and deuterium oxide (D₂O) (Cortecnet) as the solvent. The disappearance of the signals corresponding to the methacrylic protons was followed and compared with the signal of the internal standard.

The equation used to calculate the fractional conversion of the monomer was the following:

$$X_{SFOM} = 100 - \frac{(A_{db}/A_{BTC})_t}{(A_{db}/A_{BTC})_{t_0}} * 100 \quad (2)$$

Where A_{db} represents the signal area of the double bonds for polymer, and A_{BTC} represents the signal area for the internal standard, BTC. X_{SFOM} is the fractional conversion of the monomer. The sub index 0 and t indicate initial time and time t, respectively.

The gel fraction was measured by Soxhlet extraction. Vacuum dried samples were kept under continuous extraction with tetrahydrofuran (THF) (Sigma-Aldrich, purity $\geq 99.9\%$) for 24 hours. Figure 17 represents the process.

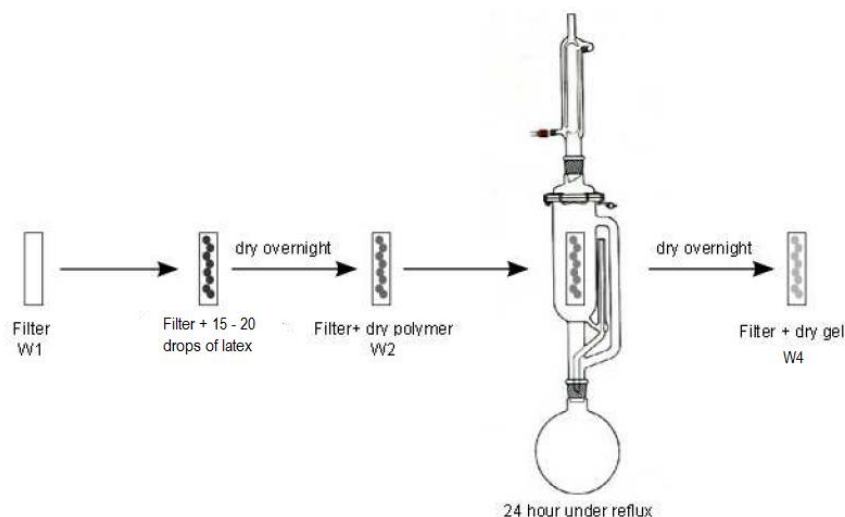


Figure 17 - Scheme of soxhlet extraction method for gel content.

To measure the gel content, glass fiber square pads (CEM) were used as backing. A few drops of latex were placed on the filter (filter weight= W_1) and dried at 60 °C for 1 hour. The filter together with the dried polymer was weighed (W_2) and a continuous extraction with THF under reflux in the Soxhlet for 24 hours was done afterwards. After this period of time, the wet filter was weighed (W_3) and dried overnight. Finally, the weight of the dry sample was taken (W_4).

The gel content was calculated as the ratio between the non-extracted dry polymer and the initial amount of dry polymer, as equation (3) shows:

$$Gel\ Content\ (\%) = \frac{W_4 - W_1}{W_2 - W_1} * 100 \quad (3)$$

The weight-average molecular weight of the sol fraction (MW, sol) was determined by Size Exclusion Chromatography (SEC). The samples taken out from the soxhlet were first dried, then, redissolved in THF to achieve a concentration of about 0.1 g/mL and finally filtered (polyamide filter $\phi = 0.45\mu\text{m}$) before injection into the SEC instrument. The setting consisted of a pump (LC- 20A, Shimadzu), an autosampler (Waters 717), a differential refractometer (Waters 2410), and three columns in series (Styragel HR2, HR4, and HR6, with pores sizes ranging from 102 to 106 Å). The analysis was performed at 35 °C using a THF flow rate of 1 mL/min. The molecular weights were relative to polystyrene as the equipment was calibrated using polystyrene standards.

Differential Scanning Calorimetry (DSC) as well as Modulated Differential Scanning Calorimetry (MDSC) were used to measure the glass transition temperature of the polymers. The same calorimeter was used to perform these analyses (Q2000 TA Instruments).

The polymer films were prepared by casting the latexes onto silicone rectangular molds and then they were dried at 22 °C and 55 % relative humidity over 7 days. A water-emulsifiable, nonylphenolic ethoxylate-free drier (Additol VXW 6206, Cytec, Belgium) was used as a catalyst for the alkyd crosslinking reaction. The metal content of the drier, which includes 5 wt. % Co, 0.22 wt. % Li, and 7.5 wt. % Zr, is commonly used in alkyd formulations. The drier was added at 2 wt. % (measured on the polymer weight) followed by stirring for 1 hour to achieve a uniform drier dispersion. After that time, the latexes were put into silicone molds and let it dried at the conditions outline above. The polymer films were carefully peeled from the silicone substrate, obtaining a rectangular film. The final thickness was about 400 µm.

Tensile mechanical properties of the films were measured in a Texture Analyzer equipment (Stable Micro Systems™).

The tested samples were rectangular: 1 mm thick, approximately, 4 mm wide and 25 mm long (length between clamps). All the tests were performed at room temperature. The crosshead speed was 1.5 mm/s corresponding to an initial strain rate of 0.1 s⁻¹. The sample was subjected to a controlled tension until failure.

4.2. Results and discussion

4.2.1 Miniemulsification

The Table 7 shows the droplet size after sonication and homogenization for the ratio SFOM:BA of 70:30.

Table 7 - Droplet size after the homogenization devices (Ratio SFOM:BA 70:30)

Synthesis	Monomer	Ratio (SFOM:BA)	dd (nm) after sonication	dd (nm) after homogenization
A	ASFOM1	70:30	154	118
B	BSFOM2	70:30	191	149
C	CSFOM4	70:30	136	124

Narrower droplet size distribution was achieved after applying high pressure homogenization, as Figure 18 represents.

During the homogenization, the droplet size decrease with the number of cycles and it is already demonstrated that 5 cycles was the minimum number of cycles needed to reach the minimum droplet size.^[9]

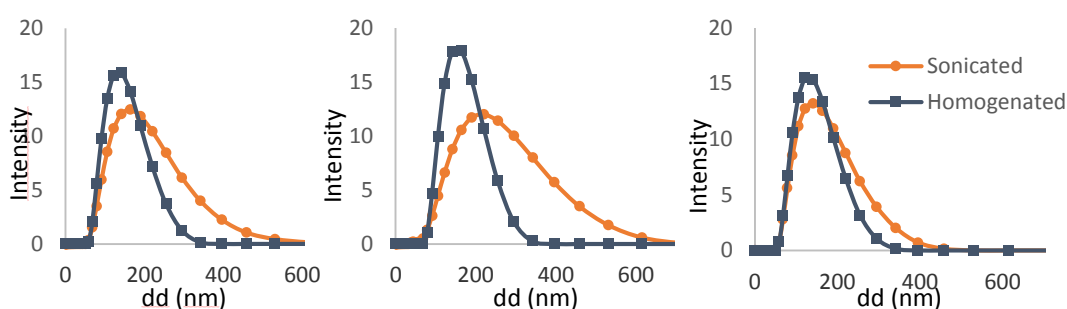


Figure 18 - Effect of the high pressure homogenization in the droplet size distribution of the miniemulsion for the synthesis A, B and C, respectively.

As Figure 18 demonstrates, using the sonication by itself it is not effective enough to get narrow droplet sizes. Thus the homogenization is essential to obtain a more homogenous mixture, especially with this kind of viscous system and even though, all the synthesis present the same behavior.

As can be seen in Figure 19, after homogenization the mixture turn out to be more homogenous and lighter.



Figure 19 - Miniemulsion of CSFOM4 after sonication and homogenization, respectively.

Table 8 shows the different ratio used and the droplet size after the homogenization devices, when the ratio of butyl acrylate was different.

Synthesis	Monomer	Ratio (SFOM:BA)	dd (nm) after sonication	dd (nm) after homogenization
B	BSFOM3	65:35	174	128
C	CSFOM5	50:50	93	69

The same behavior with the droplet size occurred. After the homogenization the droplet size is narrower.

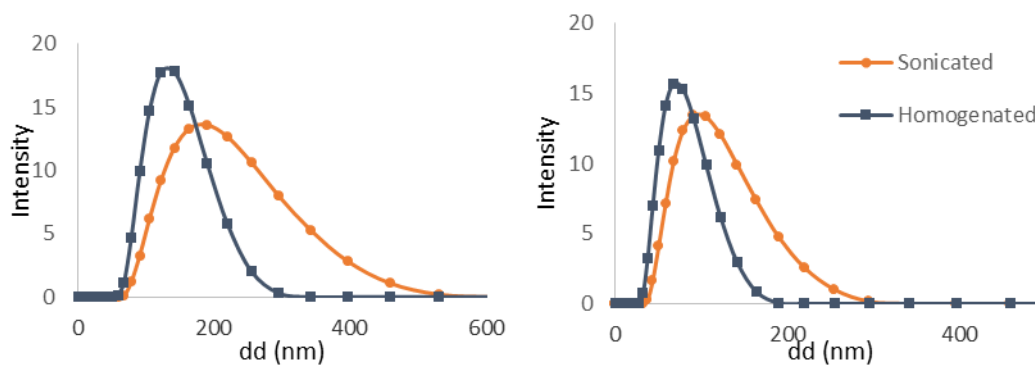


Figure 20 - Effect of the high pressure homogenization in the droplet size distribution of the miniemulsion for the synthesis B and C, respectively.

Comparing both syntheses in Figure 20, the synthesis of C gives a narrower distribution. This occurs because a higher amount of butyl acrylate was added, making the system more fluid, allowing the particles to circulate easily and passing through the sonication tip more often, making them smaller. Thus the homogenization of the mixture easily occurs, due to the less friction between the particles, obtaining a narrower distribution.

The homogenization of the homopolymer turned out to be inefficient due to high viscosity, compared with the other miniemulsions.

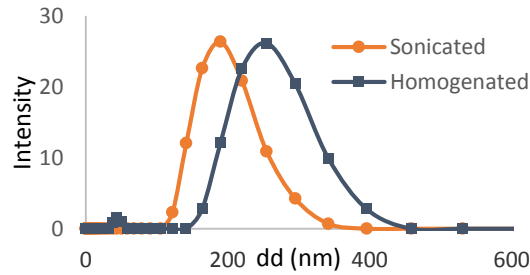


Figure 21 - Effect of the high pressure homogenization in the droplet size distribution of the miniemulsion for the homopolymerization.

In this case the homogenization was very difficult. The sunflower oil monomer is very viscous and even added to the aqueous phase, the homogenization turn out to be not as efficient as in the other miniemulsifications, as Figure 21 represents.

4.2.2 Miniemulsion Polymerization

After the preparation of the miniemulsions, miniemulsion polymerization was proceeded. During miniemulsion polymerization the evolution of the conversion degree and the particle size (dp) was investigated. Table 9 present a summary of the obtained results.

Table 9 - Summary of the final results obtained for the miniemulsions formulations employed.

Polymer	Monomer	Monomer Ratio (SFOM:BA)	Solids Content (%)	dp (nm)	Conversion (%)	Coagulum (%)
PASFOM1	ASFOM1	70:30	30	129	86	0.3
PBSFOM2	BSFOM2	70:30	30	157	90	-
PBSFOM3	BSFOM3	65:35	30	148	88	-
PCSFOM4	CSFOM4	70:30	30	148	94	0.46
PCSFOM5	CSFOM5	50:50	30	73	98	1.3
PCSFOM6	CSFOM6	100:0	10	164	98	-

At the end of some reactions coagulum was formed. In Figure 22 is represented the type of coagulum after the reactions (PCSFOM4).



Figure 22 - Coagulum in the reactor and in the agitator (PCSFOM4).

In Figures 23 and 24 is presented the evolution of the conversion degree for PASFOM1, PBSFOM2 and PCSFOM4 (ratios 70:30) during the polymerization time and the evolution of the particle size.

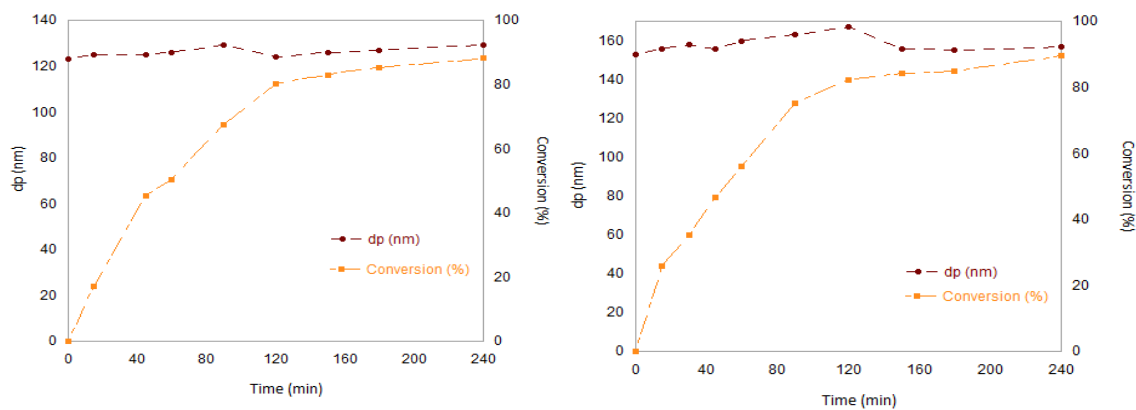


Figure 23 - Evolution of the conversion and the particle size for the polymers PASFOM1 and PBSFOM2 respectively.

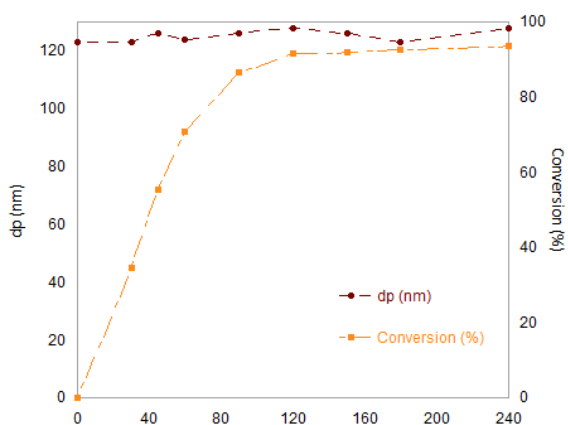


Figure 24 - Evolution of the conversion and the particle size for the polymers PCSFOM4.

It can be seen that all the polymerizations present the same behavior. For calculation of the conversion degree during the polymerization, was used $^1\text{H-NMR}$ analysis and BTC was used as internal standard.

In synthesis A, the conversion is 86%. This is justified because the monomer only presents one active site, leading to a slower polymerization.

Figure 25 represents the evolution of the $^1\text{H-NMR}$ spectra's during the polymerization time using the monomer PCSFOM4.

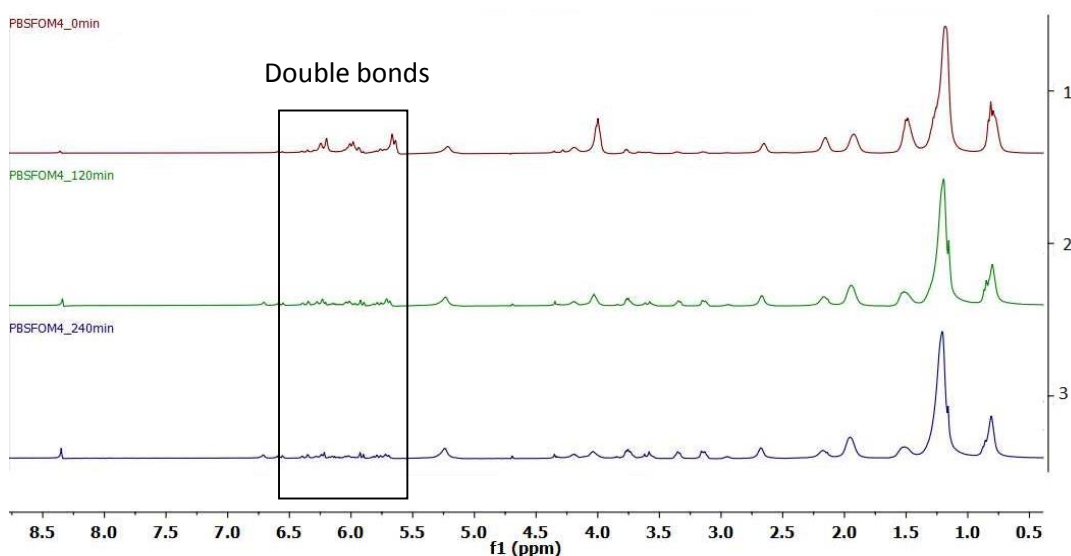


Figure 25 - $^1\text{H-NMR}$ spectra's of PCSFOM4 polymerization at different reaction times. 1) 0 minutes; 2) 120 minutes; 3) 240 minutes.

The acrylate region (5.59-6.43 ppm) corresponds to the double bonds of the copolymer (butyl acrylate and the CSFOM). During the reaction, the BTC peak (8.35 ppm) remains approximately constant, because the concentration is always the same, which doesn't happen with the latex. The depletion of the protons of the acrylate region peaks confirm the conversion of the monomer. The same behavior happened with the other reactions (Ratio 65:35 and ratio 50:50). Also, for these reactions, particle size remains constant during the polymerization and high conversions were achieved as showed in Figure 26.

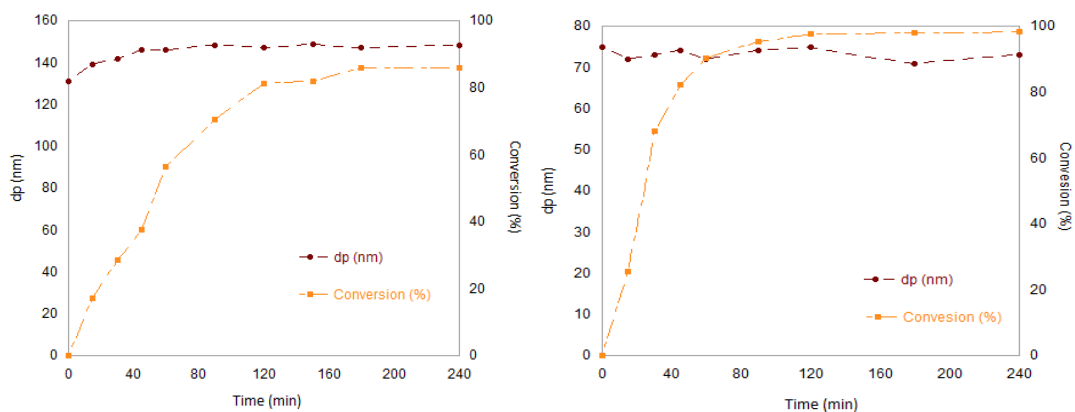


Figure 26 - Evolution of the conversion and the particle size for the polymers PBFOM3 (ratio 65:35) and PCSFOM5 (ratio 50:50), respectively.

As Figure 27 represents, for the homopolymerization, the particle size slightly varies, because of the homogenization that was not as efficient as in the other miniemulsions. High conversion was achieved after 30 minutes of reaction. The final conversion obtained was 98%.

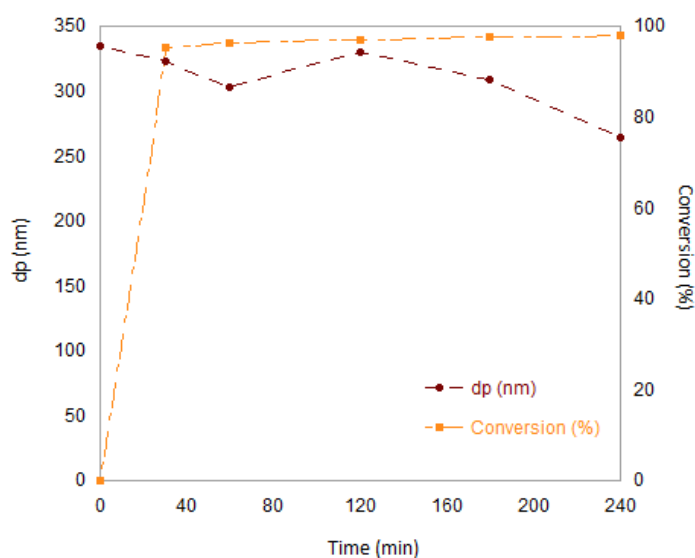


Figure 27 - Evolution of the conversion and the particle size for the homopolymer PCSFOM6.

The evolution of the particle size of all the latexes during the polymerization time remained relatively constant and close to the size of the miniemulsion droplets during the whole process.

In Figure 28 it can be seen the final latexes synthesized with the 3 different monomers.

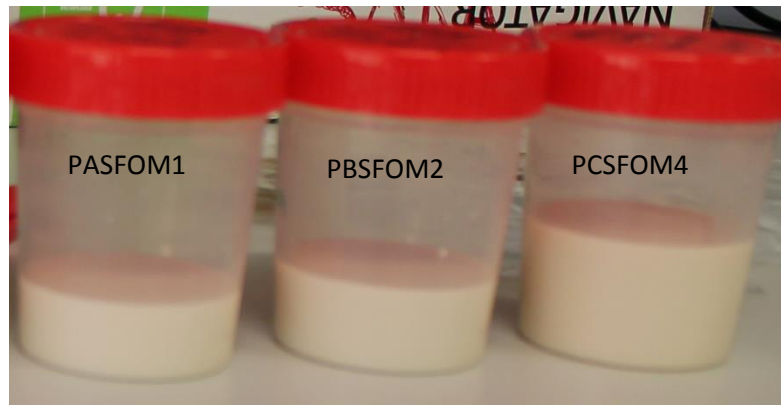


Figure 28 - Final aspect of latexes.

- Reproducibility of the reactions

In this topic, the reproducibility of the reactions will be presented for the synthesis B and C. Each reaction performed presented similar reproducibility, despite the final conversion slight changes.

Synthesis B

With this synthesis, reactions with the ratios 70:30 and 65:35 were performed. In Figure 29 the reproducibility of the polymer PBSFOM2 (ratio 70:30) is represented, and in the table 10 is the final characteristics of the polymers.

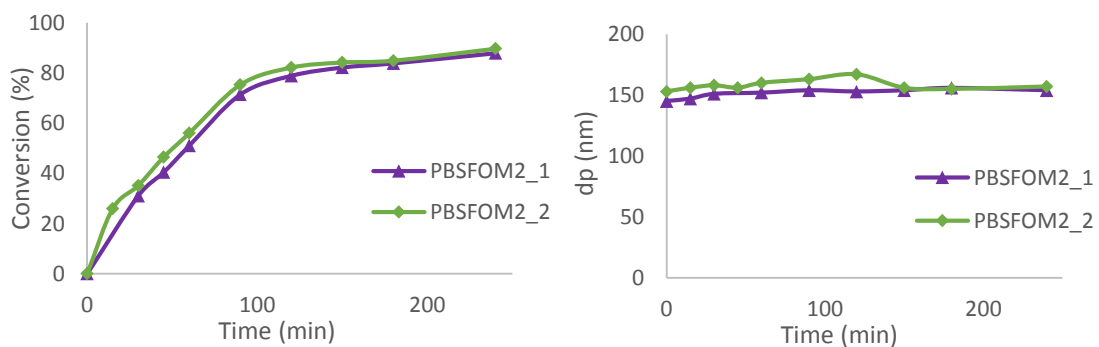


Figure 29 - Reproducibility of PBSFOM2 (ratio 70:30), for the conversion and for the particle size, respectively.

Polymer	dp (nm)	Conversion (%)
PBSFOM2_1	154	88
PBSFOM2_2	157	90

It can be seen that the reactions present the same behavior. During the reactions, the conversion was quite similar and the final conversion was almost the same. The droplet size slight varies but the final droplet size was relatively similar.

Figure 30 represents the reproducibility for the polymer PBSFOM3 (ratio 65:35) and the table 11 gives the final characteristics of the polymers.

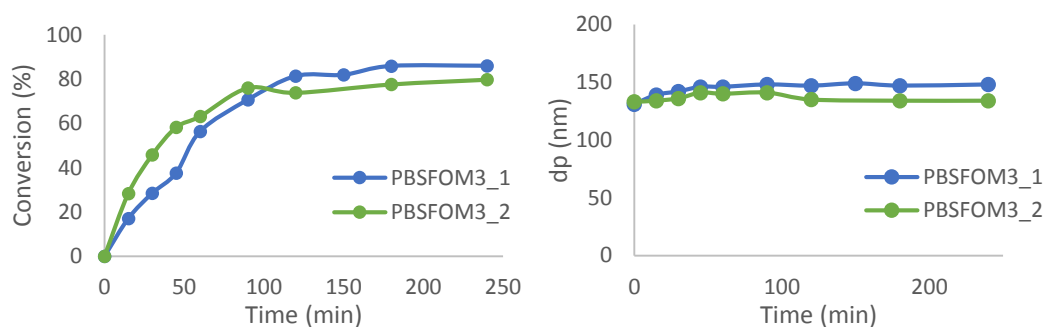


Figure 30 - Reproducibility of PBSFOM3 (ratio 65:35), for the conversion and for the particle size, respectively.

Polymer	dp (nm)	Conversion (%)
PBSFOM3_1	148	88
PBSFOM3_2	134	80

In this case, with the ratio 65:35, the reactions presented some differences, especially in the conversion during the reaction. However the final conversion was similar. Relatively to the particle size, PBSFOM3_2 presented a lower particle size than PBSFOM3_1, but both remained constant during the reaction.

Synthesis C

With this synthesis, the reactions with the ratio 70:30 were performed. Figure 31 shows the reproducibility of the polymer PCSFOM4.

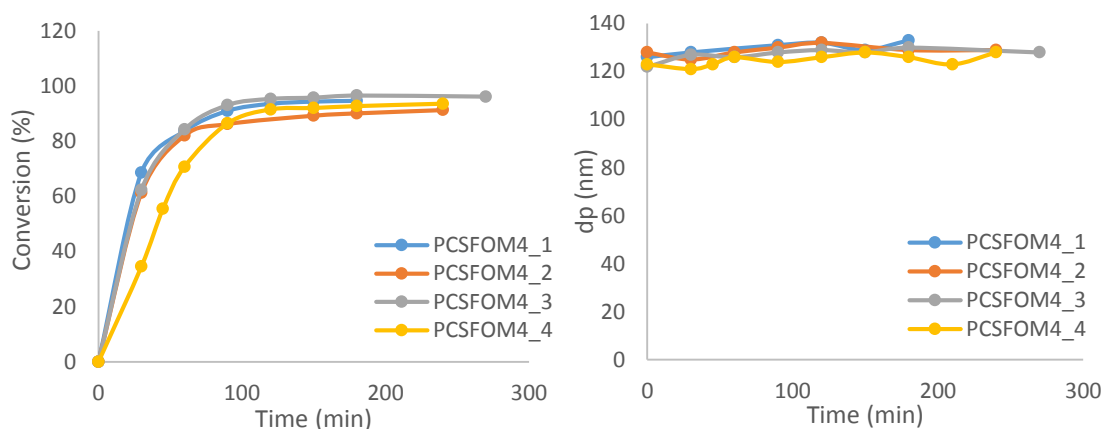


Figure 31 - Reproducibility of PBSFOM4, for the conversion and for the particle size, respectively.

Table 12 show the main characteristics of the polymer PCSFOM4.

Table 12 - Final droplet size and conversion for the PCSFOM4.

Polymer	dp (nm)	Conversion (%)
PCSFOM4_1	132	95
PCSFOM4_2	129	91
PCSFOM4_3	128	96
PCSFOM4_4	128	94

With this synthesis, all the reactions presented similar behavior between them, which indicates that the reactions produced can be reproducible.

- Gel content and Tg

In Table 13 is possible to observe that the polymers with higher values of gel content were the ones performed with the synthesis C. This take place due to the higher amount of MA added, and consequently the amount of 2-HEA, leading to have more double bounds in the final monomer structure which will lead to a very cross-linked system and

the insoluble fraction of the polymer will be retained in the soxhlet extraction filter giving us the gel content.

Table 13 - Gel content for the latexes studied.

Polymer	Monomer	Monomer Ratio (SFOM:BA)	Gel content (%)	Real Solids Content (%)
PASFOM1	ASFOM	70:30	49	31.49
PBSFOM2	BSFOM	70:30	61	31.50
PBSFOM3	BSFOM	65:35	56	31.47
PCSFOM4	CSFOM	70:30	77	31.53
PCSFOM5	CSFOM	50:50	85	31.61
PCSFOM6	CSFOM	100:0	61	10.87

Despite several attempts to measure the molecular weight of the polymers, it was not possible. After drying the polymer, it was not soluble again in THF and because of that, it couldn't be injected in the SEC instrument with the risk of clogging the columns.

Several attempts to measure this value were made, even try to dissolve the polymeres in DMF, but the polymeres weren't soluble as well.

With the chemical structure of this system, higher molecular weights should be expected, however no values were obtained.

The Tg of the polymers and the homopolymer were first tried to be measured by differential scanning calorimetry (DSC, Q2000 TA Instruments). However, no clear transitions were detected, likely because of the high crosslinking degree of the polymers, which resulted in a restriction of polymer chains mobility. Therefore, modulated DSC (MDSC, Q2000 TA Instruments) was used in an attempt to visualize the transition of the homopolymer. The final homopolymer shows a Tg equals 17 °C.

4.3. Mechanical properties

In this section the mechanical properties of the films with the polymers above described are presented. The latexes were placed in silicone molds and let it be dried for 7 days. The mechanical properties were measured after the latexes were dried at room temperature (22 °C and 55% relative humidity) and after that they were kept in the oven at 120 °C for 1 hour.

Vegetable oils contain natural antioxidants which inhibit oxidation through radical scavenging reactions. When the antioxidants are consumed, oxygen will abstract allylic hydrogen atoms creating resonance stabilized allylic radicals. Oxygen uptake and hydroperoxide formation are accompanied by an increase in the degree of double bond conjugation. The resultant allylic radicals quickly react with oxygen to form peroxy radicals. Secondary oxidation occurs next, characterized by loss of unsaturation and C-C and C-O-C bond formation via peroxide decomposition leading to radical recombination and double bond addition reactions.

Metal driers accelerate auto-oxidation by decreasing the activation energy for hydroperoxide decomposition via redox mechanisms. Primary and secondary oxidation is illustrated in Figures 32 and 33, respectively. [20, 25, 26]

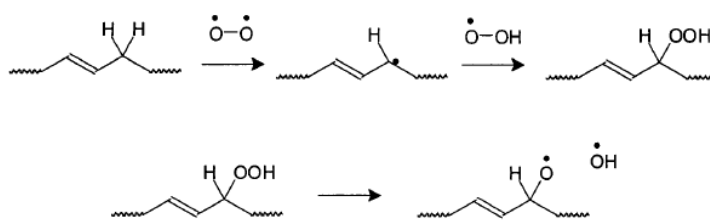


Figure 32 - Primary auto-oxidation reaction mechanism.

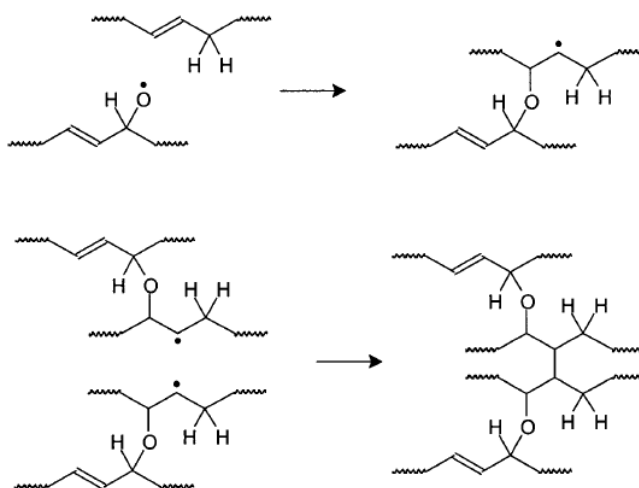


Figure 33 - Secondary auto-oxidation reaction mechanism.

As discussed before, vegetable oils macromonomers (VOMMs) possess unique characteristics such as acrylate groups, alkyl moieties, and unsaturation. The acrylate group facilitates VOMM incorporation into the polymer backbone, the alkyl moieties

provide internal plasticization during film formation, and the residual unsaturation provides oxidative cure after application and exposure to air.^[17]

The mechanical properties of the final latex film are influenced by the cross-linked fraction of the latex. For example, the higher the gel content in the latex, the higher the stiffness or toughness of the film.^[23, 24]

- Ratio 70:30

In Figure 34 are represented the dried films after 7 days for the three synthesis.

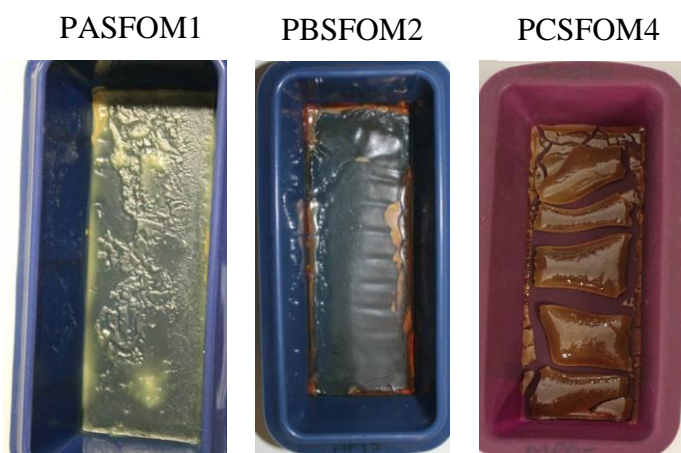


Figure 34 - Pictures of the films corresponding to the synthesis A, B and C, respectively.

The film PASFOM1 doesn't present a good film formation. It can be seen that with this monomer synthesis, the film is not either homogeneous or bright. However, the film presented some tack at touch.

The PBSFOM2 and PCSFOM4 films are homogeneous, however, the PCSFOM3 present fissures. All of the films were very bright, however the last ones didn't present any type of adhesion. (Appendix II).

- Ratios 65:35 and 50:50

In Figure 35 are represented the pictures of the films PBSFOM3 and PBSFOM5.

PBSFOM3



PCSFOM5



Figure 35 - Pictures of the films corresponding to the synthesis B and C, respectively.

This films are homogenous however the PCSFOM5 present some fissures. Despite varying the ratio, the films continued to be easily breakable, but they were a little bit stronger than the previous ones, even at room temperature. Also, they didn't present any type of adhesion. (Appendix II).

For the homopolymerization, the film was completely broken as Figure 36 shows. The absent of BA makes the film poor in adhesion but very strong in terms of stress. (Appendix II).



Figure 36 – Picture of the homopolymer PCSFOM6.

Table 14 summarize the mechanical properties of all the films. Elongation at break, Young's modulus and tensile strength are represented.

Table 14 - Mechanical properties for all the latexes.

Polymer	Monomer Ratio (SFOM:BA)	Temperature (°C)	Young's Modulus (MPa)	Tensile Strength (MPa)	Elongation at break (%)
PASFOM1	70:30	RT	0,2 ± 0,01	0,10 ± 0,01	13,26 ± 0,3
		120	1,39 ± 0,05	0,29 ± 0,02	11,04 ± 0,6
PBSFOM2	70:30	RT	0,015 ± 0,0	0,38 ± 0,04	19,20 ± 0,7
		120	0,03 ± 0,01	0,88 ± 0,02	26,08 ± 0,5
PBSFOM3	65:35	RT	0,01 ± 0,0	0,25 ± 0,1	21,39 ± 0,6
		120	0,02 ± 0,0	0,74 ± 0,2	28,00 ± 0,8
PCSFOM4	70:30	RT	0,06 ± 0,01	0,74 ± 0,3	19,72 ± 0,4
		120	0,1 ± 0,01	1,65 ± 0,5	22,75 ± 0,9
PCSFOM5	50:50	RT	0,025 ± 0,0	0,285 ± 0,1	12,88 ± 0,04
		120	0,03 ± 0,0	1,08 ± 0,3	30,87 ± 0,2
PCSFOM6	100:0	120	0,72 ± 0,2	6,45 ± 0,3	23,45 ± 0,3

In general, all the latexes at room temperature does not have good mechanical properties, however, when the latexes were submit to higher temperature, they improved.

The tensile strength and the Young's modulus were low when the films were cast at room temperature, whereas when the films were dried at 120 °C for 1 h, an important improvement on the mechanical properties in terms of strength and hardness was observed.

Despite the bad film formation, the Young's modulus in PASFOM1 at 120 °C is higher than all of the films.

Between the latexes polymerized with the synthesis B and C, the homopolymer (PCSFOM6) was very rigid and the Young's modulus was very high comparing with the other latexes. The increase at the tensile strength and Young's Modulus in this latex was notable. Their properties, improved, making the sunflower oil monomer a good raw material to form strong and hard films.

The difference between the latexes PASFOM1, PBSFOM2 and PCSFOM4 (ratio 70:30) and the PBSFOM3 and PCSFOM5 (ratio 65:35 and 50:50, respectively) was not significant. The PBSFOM3 and PCSFOM5T have a higher value of elongation at break, which make them a little stiffer.

The polymers which present higher amount of gel content, were the ones with higher values of stress and strain (Young's Modulus), and tensile strength (synthesis C), this means that the films were stiffer than the other ones and present a higher resistance when subject at force.

Chapter 5

Conclusions

In this work, three different monomers were functionalized, varying the amount of maleic anhydride (molar ratio used based on the percentage of linoleic acid present in the sunflower oil). It was proved that the molar ratio of 1:1 does not provide a good film formation neither good mechanical properties. Thus the synthesis C (molar ratio 1:2) was the one which present the best results, not in the film formation, but it was the one with better tensile strength results.

The polymerization turns out to be efficient and higher conversions were obtained. Also all the reactions can be reproducible, which makes this system very able to produce similar results.

Unfortunately, due to the extreme cross-linked system, it was not possible to measure the Tg of the polymers.

Also the molecular weight can neither be measured because the polymer was not resolvable in THF. Several attempts to measure this value were made, also changing the solvent, but the polymers continued to be insoluble.

During the film formation, brittle films with low mechanical properties were obtained. The SFO monomer should be functionalized with a ratio of SFO: MA between 1:1.5 and 1:2, in order to, after the polymerization, provide a good film formation. With the aim of obtaining films with higher amount of SFOM, we figure out that stable polymer latexes could be obtained by copolymerization of BA: SFOM with 30% solids content and in a ratio of 30:70. The polymer films obtained by drying of the latexes showed low mechanical properties. All the films presented to be very brittle, but an improvement of this properties were verified when the films were kept in the oven at 120°C for 1 hour.

Future work

In a future investigation, the copolymerization with other acrylates should be elucidated. It is also necessary to carry out a further investigation to characterize the final products obtained and try to improve the mechanical properties and also verify the adhesive

properties of them. During the film formation, it should also be investigated the curing of the films for more days.

Several trials should be made in order to change the percentage of the additol added in the reactions performed to see if the films formed continue to have cracks.

Bibliographic References

- [1] Bierman, U.; Bornscheuer, U.; Meier, M. A. R.; Metzger, J. O.; Schafer, H. J. *New Synthesis with Oils and Fats as Renewable Raw Materials for the Chemical Industry*, *Angew. Chem. Int.*, **2000**, 39,2206-2224.
- [2] Schubert, U. S.; Metzger, J. O.; Meier, M. A. R. *Plant oil renewable resources as green alternatives in polymer science*, *Chem. Soc. Rev.*, **2007**,36, 1788-1802.
- [3] Xia, Y.; Larock, R. C. *Vegetable oil-based polymeric materials: synthesis, properties, and applications*, *Green Chem.*, **2010**, 12, 1893-1893.
- [4] Espinosa, L. M.; Ronda, J. C.; Galià, M.; Cádiz, V. *A New Route to Acrylate Oils: Crosslinking and Properties*, of Acrylate Triglycerides from High Oleic Sunflower Oil, *Journal of Polymer Science Part A: Polymer Chemistry* **2009**, Vol. 47, 1159–1167.
- [5] Ronda, J. C.; Lligadas, G.; Galià, M.; Cádiz, V. *Vegetable oils as platform chemicals for polymer synthesis*, *European Journal of Lipid Science and Technology* **2011**, 113, 46-58.
- [6] Khot, S. N.; Lascala, J. J.; Can, E.; Morye, S. S.; Williams, G. I.; Palmese, G. R.; Kusefoglu, S. H.; Wool, R. P. *Development and Application of Triglyceride-based Polymers and Composites*, *Journal of Applied Polymer Science* **2001**, 82 (3), 703-723.
- [7] Güner, F. S.; Yağci, Y.; Erciyes, A. T. *Polymers from triglycerides oils*, *Progress in Polymer Science* **2006**, 31, 633-670.
- [8] Asua, J. M. “*Miniemulsion polymerization*”, *Progress in Polymer Science*, **2002**, 27, 1283-1346.

- [9] Quintero, C.; Mendon, S. K.; Smith, O. W.; Thames, S. F. *Miniemulsion polymerization of vegetable oil macromonomers*, Prog. Org. Coat, **2006**, 57, 195-201.
- [10] Report of the United Nations Conference on Environment and Development, Rio de Janeiro, 1992; <http://www.un.org/esa/sustdev>.
- [11] Gandini, A.; Belgacem, M. N. *Monomers, Polymers and Composites from Renewable Resources*. Elsevier: Amsterdam, **2008**.
- [12] Espinosa, L. M.; Meier, M. A.R. *Plant oils: The perfect renewable resource for polymer science?!*, European Polymer Journal 47, **2011**, 837–852.
- [13] Moreno, M. *Waterborne Polymers based on Sunflower Oil Fatty Acids*, PhD Thesis, 264 pages, University of the Basque Country (UPV/EHU), **2013**
- [14] Bloor, W. R. Biochemistry of the Fats, *Chemical Reviews* **1925**, 2, 243-300.
- [15] Gorkum, R.; Bouwman, E. The oxidative drying of alkyd paint catalyzed by metal complexes, *Coordination Chemistry Reviews* **2005**, 249, 1709-1728.
- [16] Vilela, C. A. C. *Synthesis of new vegetable oil-based polymeric materials*, PhD Thesis, 220 pages, Universidade de Aveiro (**2012**).
- [17] Bunker, S. P.; Wool, R. P. *Synthesis and characterization of monomers and polymers for adhesives from methyl oleate*, Journal of Polymer Science Part A: Polymer Chemistry **2002**, 40 (4), 451-458.
- [18] Etxebarria, A. A. *Waterborne PSAs for Low Energy Surfaces*, PhD Thesis, 211 pages, University of the Basque Country (UPV/EHU), (**2011**).
- [19] Elorza, A. L. *Design and Production of Waterborne Polyurethane/Acrylic Hybrid Pressure Sensitive Adhesives*, PhD Thesis, 331 pages, University of the Basque Country (UPV/EHU), (**2008**).

- [20] Black, M. S. Reactivity of Vegetable Oil Macromonomers in Thiol-ene, Cationic and Emulsion Polymerizations, PhD Thesis, 234 pages, The University of Southern Mississippi, **2007**.
- [21] Johnson, L. F.; Schoolery, J. N. *Determination of Unsaturation and Average Molecular Weight of Natural Fats by Nuclear Magnetic Resonance*, Anal. Chem, **1962**, 34, 1136-1139.
- [22] Rodriguez, R. *Silicone-Modified Acrylic Nanoparticles by Miniemulsion Polymerization*, PhD Dissertation, University of the Basque Country, Spain, **2007**.
- [23] Back, A. L. *Relation between Gel Content, Plasticity, and Dilute Solution Viscosity of Elastomers*, Ind. Eng. Chem, **1947**, 39, 1339-1343.
- [24] Członkowska-Kohutnicka, Z.; Raszczuk, A. *Effect of microgels on the viscoelastic properties of poly (dimethylvinylsiloxanes)*, Appl. Polym. Sci, **1975**, 19, 1269-1273.
- [25] Mallégo, J.; Lemaire, J.; Gardette, J. L. *Drier influence on the curing of linseed oil*, Progress in Organic Coatings, **2000**, 39, 107-113.
- [26] Johansson, M.; Stenberg, C.; Svensson, M. *Study of the drying of linseed oils with different fatty acid patterns using RTIR-spectroscopy and chemiluminescence (CL)*, Industrial Crops and Products, **2005**, 21, 263-272.
- [27] Moreno, M; Goikoetxea, M; Barandiaran, M. *Biobased-Waterborne Homopolymers from Oleic Acid Derivatives*, Institute for Polymer Materials (Polymat) and Chemical Engineering Group, University of the Basque Country (UPV/EHU), Joxe Mari Korta Center, 20018 Donostia-San Sebasti_an, Spain.

- [28] Manea, M.; Chemtob, A.; Paulis, M.; de la Cal, J. C.; Barandiaran, M. J.; Asua, J. M. *Miniemulsification in High-Pressure Homogenizers*. *AIChE Journal* **2008**, *54* (1), 289-297.
- [29] Lopez, A.; Degrandi-Contraires, E.; Canetta, E.; Creton, C.; Keddie, J. L.; Asua, J. M. *Waterborne Polyurethane–Acrylic Hybrid Nanoparticles by Miniemulsion Polymerization: Applications in Pressure-Sensitive Adhesives*. *Langmuir* **2011**, *27* (7), 3878-3888.
- [30] Rodriguez, R. *Silicone-Modified Acrylic Nanoparticles by Miniemulsion Polymerization*. PhD Dissertation, University of the Basque Country, Spain, **2007**.
- [31] Taylor, P. *Ostwald Ripening in Emulsions*. *Advances in Colloid and Interface Science* **1998**, *75* (2), 107-163
- [32] Higuchi, W. I.; Misra, J. *Physical Degradation of Emulsions Via the Molecular Diffusion Route and its Possible Prevention*. *J. Pharm. Sci.* **1962**, *51*, 459-466.

Appendix

Appendix I. Processes and characterization methods

I.1. Droplet and particle sizes

The droplet and particle size and droplet and particle size distribution (PSD) were measured by dynamic light scattering (Nanosizer, Malvern). The equipment determines the particle size by measuring the rate of fluctuations in laser light intensity scattered by particles as they diffuse through a fluid.

Samples were prepared by diluting a fraction of the miniemulsion or latex in distilled water, saturated with monomers in the case of miniemulsion droplets in order to avoid droplet destabilization by thermodynamic reasons. The analysis was carried out at 25 °C and a run consisted in 1 minute of temperature equilibration followed by 2 size automatic measurements.

I.2. Polymerization reactors

The polymer latexes were synthesized in batch by miniemulsion polymerization at 70 °C. Small scale reactions were carried out in the Miniplant M100 setup (Chemspeed Technologies) 4 in stainless steel reactors of 100 mL. The reactor head includes an integrated reflux condenser, sampling device, nitrogen inlet and its own syringe pump providing semi continuous flow of liquids. A stainless steel turbine-type stirrer rotating at 150 rpm was used (Figure I.1)



Figure I.1 - Representation of stainless steel Chemspeed reactors.

I.3. Monomer Conversion

Monomer conversion was measured by $^1\text{H-NMR}$ spectroscopy. Samples were recorded using a 500 MHz $^1\text{H-NMR}$ BrukerDRX-500 spectrometer.

The addition to the sample of 1,3,5-benzenetricarboxylic acid (BTC) as internal standard allows the determination of the absolute concentration of residual monomer by means of a calibrate. Thus, all the monomer concentrations were related to the BTC. To prepare the $\text{D}_2\text{O-BTC}$ solution, BTC was dissolved in NaOH 1M and then neutralized with HCl and diluted with water.

The analysis were recorded with two different conditions, in both cases the value of gain of the experiment is fixed. High monomer concentration (low conversions, number of scans=8, gain=128) and for low monomer concentration (high conversions, number of scans=32, gain=512). All the spectra were recorded in a mixture of (10:90) $\text{D}_2\text{O}/\text{H}_2\text{O}$ solution at 300 K. The samples were prepared adding 300 μL of a BTC solution in $\text{D}_2\text{O}/\text{H}_2\text{O}$, 50 μL of latex withdrawn from the reactor at the desired reaction time.

To prepare the $\text{D}_2\text{O-H}_2\text{O-BTC}$ solution, 0.1250 g of BTC was dissolved in 10-15 mL of 1 M NaOH . Then, the solution was neutralized with HCl and diluted to 25 mL with $\text{H}_2\text{O}+\text{D}_2\text{O}$. The final concentration of BTC was $5 \times 10^{-3} \text{ gmL}^{-1}$. The spectra were recorded using the sequence WATERGATE to suppress the signal of water. This technique allows the analysis of the sample immediately after being withdrawn from the reactor.

Appendix II. Mechanical Properties

- Synthesis A

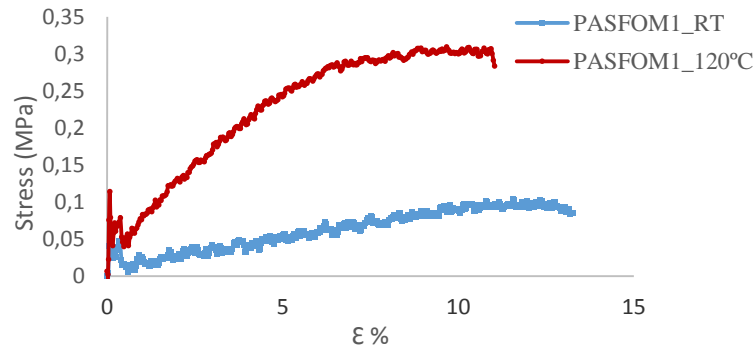


Figure II 1 - Stress and strain curves for the film PASFOM1

Due to the bad film formation, it presented to be a very brittle system, as can be seen through the stress and strain (ϵ) values. However, the mechanical properties improved (red line represented in Figure 36) when the film were dried in the oven but it continued to be a very fragile film.

- Synthesis B

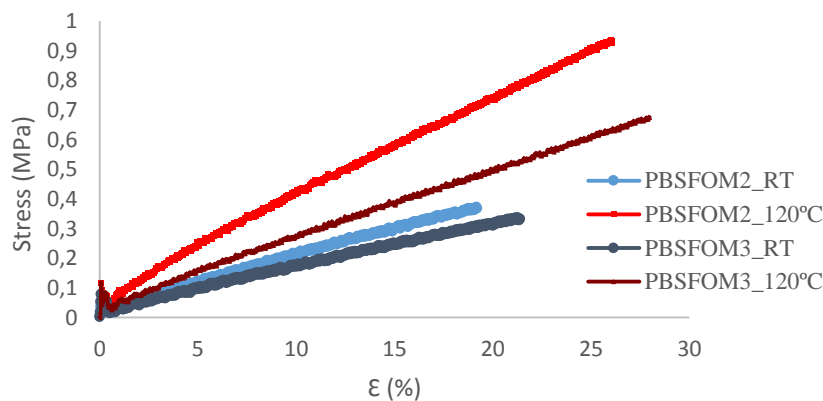


Figure II 2 - Stress and strain curves for the films PASFOM2 and PBSFOM3.

The mechanical properties improved when the films were kept in the oven, specially the stiffness, although they continue to break easily. Both films presented similar results, despite of the BA ratio in the polymer 3 were higher.

- Synthesis C

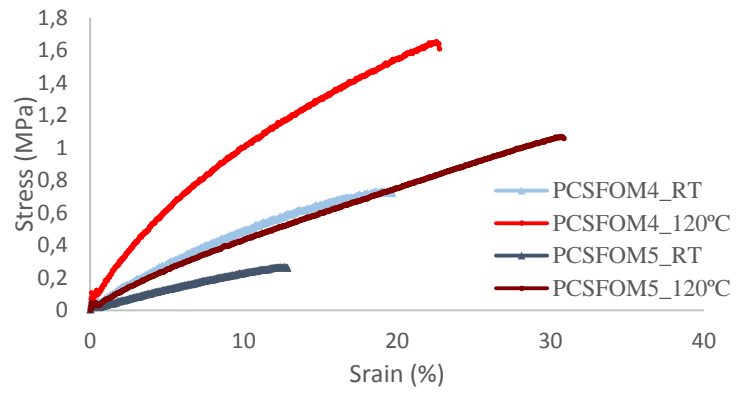


Figure II 3 - Stress and strain curves for the films PASFOM4 and PBSFOM5.

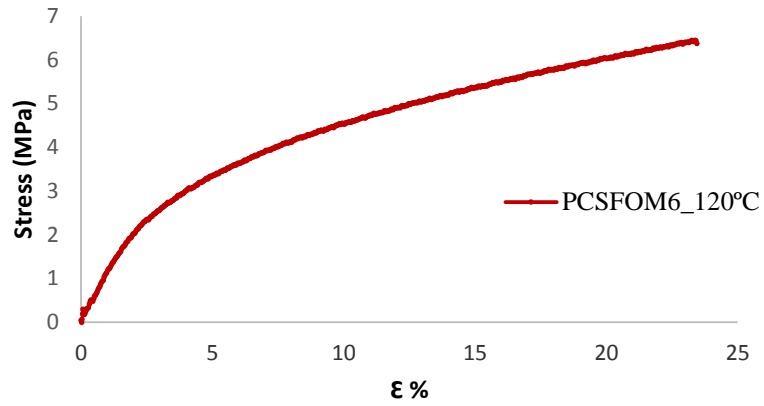


Figure II 4 – Stress and strain curve for the homopolymer at 120 °C.